Varis Žentiņš

INCREASING THE EFFICIENCY OF DISTRICT HEATING AND REPLACING FOSSIL FUELS WITH ALTERNATIVE ENERGY SOURCES (ALGORITHMS OF HEAT SOURCE PARAMETRIC OPTIMIZATION)

Summary of the Doctoral Thesis

RIGA TECHNICAL UNIVERSITY

Faculty of Mechanical Engineering, Transport and Aeronautics
Institute of Mechanics and Mechanical Engineering

Varis Žentiņš

Doctoral Student of the Study Programme "Heat Power Engineering and Heat Engineering"

INCREASING THE EFFICIENCY OF DISTRICT HEATING AND REPLACING FOSSIL FUELS WITH ALTERNATIVE ENERGY SOURCES
(Algorithms of Heat Source Parametric Optimization)

Summary of Doctoral Thesis

Scientific supervisor
Associate Professor Dr. sc. ing.
SIGURDS JAUNDĀLDERS

Cover image from the archive of "Industry Service Partner" Ltd.

DOCTORAL THESIS PROPOSED TO RIGA TECHNICAL UNIVERSITY FOR THE PROMOTION TO THE SCIENTIFIC DEGREE OF DOCTOR OF SCIENCE

To be granted the scientific degree of Doctor of Science (Ph. D.), the present Doctoral Thesis has been submitted for the defence at the open meeting of RTU Promotion Council on December 15, 2022 at the Faculty of Mechanical Engineering, Transport and Aeronautics of Riga Technical University, Ķīpsalas Street 6B, Room 521.

OFFICIAL REVIEWERS

Researcher Ph.D. Oļegs Jakovļevs,
Riga Technical University, Latvia

Dr. habil. sc. ing. Namejs Zeltiņš,
Institute of Physical Energetics, Latvia

Professor Dr. Giedrius Janušas,
Kaunas University of Technology, Lithuania

DECLARATION OF ACADEMIC INTEGRITY

I hereby declare that the Doctoral Thesis submitted for the review to Riga Technical University for the promotion to the scientific degree of Doctor of Science (Pf. D) is my own. I confirm that this Doctoral Thesis had not been submitted to any other university for the promotion to a scientific degree.

Name Surname ……………………………. (signature)
Date: ………………………

The Doctoral Thesis has been written in Latvian/English. It consists of an Introduction; 6 Chapters; Conclusion; 57 figures; 7 tables; 13 appendices; the total number of pages is 110, including / not including appendices. The Bibliography contains 105 titles.

ACKNOWLEDGEMENTS

CONTENTS

EXPLANATION OF USED TERMS AND ABBREVIATIONS

DHS – district heating system
CHP – combined heat and power
HS – heat storage
DHN – district heating network
KM – boiler house
GHG – greenhouse gases
MWh – megawatt hour
kWh – kilowatt hour
HL – heat load, MW
EU – European Union
COP – coefficient of performance
OT – outside temperature
RTU – Riga Technical University
J – joule
k – coefficient
f – number of factors
CO_2 – carbon dioxide
MPC – mandatory procurement components
MP – mandatory procurement
FGS – flue gas condenser
AHP – absorption type heat pump
h – hour
ARIMA – autoregressive integrated moving average
$C_{pp\,el}$ – production price of electricity, Eur/MWh_{el}
C_f – fuel costs, Eur/MWh
C_{pph} – production price of heat, Eur/MWh_{th}
C_{CO2} – market price of emissions CO_2, Eur/t
$C_{mp\,el}$ – market price of electricity, Eur/MWh_{el}
$C_{mp\,th}$ – market price for heat, Eur/MWh_{el}
$\overline{(Cmp)}$ – avarage market price
$\overline{(Cmp)}_{best\,max.period}$ – average electricity market price for the best period, Eur/MWh_{el}
T_{o1h}(wind, precip.) – hourly data for outdoor temperature as well as wind strength and precipitation forecast; °C, m/s, Yes/No
Q_{p1h} – heat forecast per hour, MWh
T_{1_1h} – network flow temperature per hour, °C
$T_{2\,1h}$ – network return temperature per hour, °C

$\overline{Q_{p1-24h}}$ – average predicted heat load, MWh
P_{hmax} – CHP maximum heat load capacity, MWh
$\overline{P}_{el\,max.\,ar\,HS}$ – maximum average power of CHP operation with HS, MW
$P_{el}1h$ – total electric power per hour, MW_{el}
P_{sc} – hourly electricity for own consumption, MW_{el}
P_h1h – heat hourly capacity in the electricity generation process, MW_{th}
Re^{HS} – revenue from the sale of electricity produced by CHP with HS, Eur
Re^{el} – revenue from the sale of electricity produced by CHP, Eur
Q_{hs_actual} – actual HS heat capacity, MWh
P_{hs_charge} – HS charge power, MW
$P_{hs\_discharge}$ – HS discharge power, MW
$Q_{foresc.HS}$ – forescated HS heat capacity, MWh
$P_{char(forecasted)}$ – forescated HS charge power, MW
$P_{disch(forecasted)}$ – forescated HS discharge power, MW
$C_{el.losses}$ – electrical losses during the operation of HS, Eur
$C_{heat\,losses}$ – heat loss during HS operation, Eur
C_{maint} – maintenance and repair costs of HS (losses), Eur
C_{losses} – all losses of HS, Eur
$P_{min\,gen}$ – minimum electricity generation capacity, MW
$C_{network\,el}$ – electricity price from the network, Eur/MWh_{el}
θ – dimensionless temperature
ξ – dimensionless tank height
λ – thermal conductivity
δ – dimensionless thermocline thickness
ν – kinetic viscosity
τ – dimensionless time
ρ – water density, kg/m^3
ε – correction factor
δ_0 – dimensionless height of the original thermocline
μ – dynamic viscosity, Pa·s
ω – speed field vortex function in the tank
ψ – speed field flow function in the tank
V_r – radial acceleration velocity, m/s

INTRODUCTION

Actuality of the Thesis

Improving the efficiency of the district heating system (DHS) and replacing fossil fuels with renewable energy sources is one of the key challenges for the energy sector to achieve long-term climate neutrality in the European Union (EU) by 2050 [1], [3], [5]. This political goal is not only necessary to reduce and prevent global climate change, but also has a positive effect on the security of energy supply and the competitiveness of national economies. Latvia has a well-developed DHS, and 69.5 % of the population is provided with heating and hot water [2].

The topicality of the Thesis is also justified by such adopted legislation as the new climate and energy goals set in the EU directives. Reaching of climate neutrality until 2050 is set for the interim period of 2030. In order to move closer to climate neutrality, the following renewable energy sources and energy efficiency targets were revised and raised in 2018, and in the period from 2021 to 2030 are to be met:

- reduction of at least by 40 % of greenhouse gas emissions (compared to the level of year 1990);

- at least 32 % of renewable energy;

- energy efficiency improvement at least by 32.5 % [4].

Proposals are constantly being complemented, and in December 2020, the EU leaders set a new target – *fit 55*, which forecasts the reduction of GHG emissions already by 55 % (compared to 1990) [6]. In order to meet the commitments already made and move towards the new goals, it is necessary to rebuild the entire energy sector and develop a completely new concept for district heating. There is an active research and discussion not only about the 4th generation, but also about the 5th generation district heating system concepts, which show that every element of the system can be a consumer and a producer. The use of low-potential heat with heat pump technology and the balancing of the system with heat accumulators is very important for such systems. The dissertation offers a multi-perspective analysis and develops an algorithm that allows to assess one of the main driving forces – the accumulation of heat, which would significantly accelerate the transition to the next generation of district heating systems in the future and allow fulfilling of the commitments.

Hypothesis of the Thesis

Is it possible to find optimal operating modes of a cogeneration plant using heat storage technology in the conditions of the free electricity market in order to increase efficiency and reduce fossil fuels.

The goal of the Thesis

The aim of the Doctoral Thesis is to study different modes of operation of Latvian cogeneration plants and to offer solutions for increasing their efficiency and fossil fuels under changing working conditions. To develop a calculation methodology for heat accumulation losses for operating modes and include this unit in the cogeneration plant decision-making algorithm.

Tasks of the Thesis

In order to achieve the set goal, the following tasks were set:
1. To carry out a study on the peculiarities of climate and the possibilities of increasing the efficiency of cogeneration plants. Analysis of cogeneration plants in Latvia and production decision-making in the free electricity market.
2. To increase the efficiency of the heat source work and reduce emissions. Use of an absorption type heat pump and heat accumulator.

3. To carry out research and develop a methodology for calculating heat loss in operating modes. To compare the most effective thermal insulation solutions of the 3 largest heat accumulators in Latvia according to the developed methodology.To use the experimental method for determining actual heat losses and verifying the heataccumulator.

4. To carry out a study on heat load forecasting.
5. To optimize the cogeneration plant decision-making algorithm using in-depth analysis of the heat accumulator and including the accumulator loss model.

Methodology of research

In order to achieve the aims of the Thesis, the general reference method was used in the introductory part, with the help of which the latest publications were researched, analysed and summarised. Types of heat energy accumulation and heat pumps technologies, latest trends and topicality of the theme are explored. The system dynamics research method was used to determine the factors influencing the system behaviour of the accumulation tank operation and efficiency complex. Multi-criteria analysis was performed of each factor influencing the system and was described in recent publications.

Using the method of empirical cognition, facts and information about the research objects was accumulated during the experiments. The research was performed using real operating storage equipment. Direct measurement was used to determine the actual heat loss. In order to obtain the most reliable results, the empirical observation took place under the natural conditions of the object. Actual heat losses from the experimental data analysis and calculations were determined. A mutual comparison of the experiment and theoretical calculations has been performed.

Technological efficiency evaluation for thermal insulation has been performed. The calculation methodology developed in the research allows to calculate heat losses in different operating modes and to compare the solutions. By understanding the behaviour of the heat storage system and gathering the experience of different companies, a decision-making algorithm was developed that allows to increase the overall efficiency of the plant, reduce CO_2 emissions, and replace fossil fuels.

Scientific novelty of the Thesis

The research carried out in the work shows the possibilities of cogeneration plant regime optimization using heat pump and storage equipment. Real data of heat supply companies in the climatic conditions of Latvia were used in the performed research.

As a result of the research, the cogeneration decision-making algorithm with the heat storage device is optimized, which describes the behaviour of five interconnected units (electricity cost and market price analysis, weather forecast, cogeneration modes, and heat accumulator performance parameters), which allows to study the system's feedback. Each of the blocks is described by subsystems and equations that characterize the system performance criteria and interactions. The proposed methodology allows not only for a differentiated analysis of the heat accumulator operation, but also to view the usefulness of this equipment and the possibilities of its integration into the heat supply system. An important study is the development of a heat accumulator loss calculation methodology in operating modes and the inclusion of this unit in the decision-making algorithm.

Practical significance of the Thesis

The Doctoral Thesis has been approved by one of the largest cogeneration plants in Latvia, "GREN LATVIJA" Ltd and "JUGLAS JAUDA" Ltd. Based on the research results, it will be possible to make an informed choice of investment policy not only in heat supply companies, but also in the course of developing the national energy policy to achieve the set goals.   It will help to accelerate the transition to the free

electricity and heat supply market, which is related to increasing the efficiency of the technological process and changing the production algorithm.

Structure and contents of the Thesis

The Thesis has been written in Latvian. It contains an introduction, six chapters, conclusions and recommendations, appendices, and a bibliography. It contains 59 figures and 8 tables; the total number of pages is 110. The list of literature includes 104 sources.

Chapter 1 is dedicated to the peculiarities of Latvia's climate and opportunities to increase the efficiency of cogeneration plants. It presents the analysis of cogeneration plants in Latvia and studies the state support policy and production decision-making in the free electricity market.

Chapter 2 is dedicated to the issue of increasing the efficiency of the heat source and reducing emissions, the use of an absorption type heat pump and heat accumulator. A study on heat recovery from flue gases has been performed, as well as the validity of use of the heat accumulator in the cogeneration plant production process.

Chapter 3 presents a study that has been performed and a heat loss calculation methodology for heat loss operating modes that has been developed. It compares the most effective thermal insulation solutions of the 3 largest heat accumulators in Latvia according to the developed methodology.

Chapter 4 is devoted to the use of an experimental method for determination of actual heat loss and for verification of a heat accumulator The chapter publishes the description of the experiment, information about the used measuring instruments and their accuracy, as well as the progress of the experiment planning. The obtained experimental results are compared with the theoretical calculation. Thermal bridges are detected by thermography and heat losses are calculated. Verification of the heat accumulator is performed by introducing a correction factor.

Chapter 5 is dedicated to consideration of the heat energy situation in Latvia and to heat load forecasting with heat load profile.

Chapter 6 describes optimization of the cogeneration plant decision-making algorithm using in-depth analysis of the heat accumulator and including the accumulator loss model. Analysis of the heat accumulator cost model has been performed, where losses to ensure the process have been estimated. The impact of maintenance and repair costs as well as the increase of efficiency using the asset management system is considered.

Author's personal contribution

The Thesis was developed in close cooperation with Associate Professor S. Jaundālders and other co-authors. The author participated in all stages of the research, such as data acquisition, collection of input data required for calculations and analysis of simulation results. The author developed the calculation method in Microsoft Excel, Therm and Matlab software and performed the necessary experiments with a real heat accumulator and central heating systems.

The research on heat energy accumulation is performed in the Thesis, the experience of various heat supply companies is summarized, and as a result, the author has developed his decision-making algorithm in the conditions of the free electricity market, which has been evaluated by industry companies.

Approbation of the research and publications

The main scientific achievements and results of the Doctoral Thesis have been presented at 5 international and 1 local scientific conference.
Five scientific articles have been published on the topic of the Doctoral Thesis, which are indexed in the SCOPUS database and five publications have been published in conference proceedings.

Approbation of the D**octoral** Thesis

The results of the work were reported and discussed at four international conferences.

1. RTU 59th International Scientific Conference, 12 October 2018,, Riga, Latvia.
2. 19th International Scientific Conference on Engineering for Rural Development, 20–22 May 2020, Jelgava, Latvia.
3. RTU 60th International Scientific Conference on Power and Electrical Engineering (RTUCON 2019), 7–9 October 2019, Riga, Latvia.
4. RTU 61st International Scientific Conference on Power and Electrical Engineering of Riga Technical University (RTUCON 2020), 5–6 November 2020, Riga, Latvia.
5. RTU 61st International Scientific Conference , 14 October 2020, Riga, Latvia.
6. RTU 62nd International Scientific Conference , 15 October 2021, Riga, Latvia.
7. RTU 62nd Student Scientific Conference. Section "Production Technology", 29 April 2021, Riga, Latvia.
8. Scientific Methodology Conference "Challenges in Engineering HigherEducation", 15 October 2021, Riga, Latvia.

Scientific publications

1. Soročins, A., Rusovs, D., Nagla, J., **Žentiņš V**. The Influence of the Thermal Storage on the Electricity Production in a Co-Generation in Peak and Off-Peak Time Range. *2020 IEEE 61st International Scientific Conference on Power and Electrical Engineering of Riga Technical University (RTUCON 2020)*: 5–6 November 2020, Riga, Piscataway: IEEE, 2020, pp.136–139. ISBN 978-1-7281-9511-7.

2. Soročins, A., Nagla, J., **Žentiņš V**. District Heating Simulation Model Development to Solve Optimization Problems in the Market Conditions. In*: 2020 IEEE 61st International Scientific Conference on Power and Electrical Engineering of Riga Technical University (RTUCON 2020*), Latvija, Riga, 5–6 November 2020. Piscataway: IEEE, 2020, ISBN 978-1-7281-9511-7

3. Rusovs, D., **Žentiņš, V**. Steam driven absorption heat pump and flue gas condenser applied for heat recovery in district heating network. *19th International Scientific Conference Engineering for Rural Development*. 2020, Jelgava, pp.1627–1632. ISSN 1691-5976

4. **Žentiņš, V.**, Rusovs, D., Soročins, A., Cars, A. Increasing the efficiency of the heat storage by using a absorption heat pump. *Riga Technical University 62nd International Scientific Conference.* 15 October 2021, p. 9, ISBN 978-9934-22-756-1

5. **Žentiņš, V.,** Rusovs, D., Soročins, A., Cars, A. Analysis of different thermal insulation solutions of a heat storage. *Riga Technical University 62nd International Scientific Conference.* 15 October 2021, p. 5, ISBN 978-9934-22-756-1

6. Vostrikovs, S., **Žentiņš, V.**, Rusovs, D., Klimatneitralitāte, tehnogēno risku mazināšana un atjaunojamo energoresursu izmantošana siltumapgādē un enerģētikā. *Zinātniski metodiskā konference "Izaicinājumi inženierzinātņu augstākajā izglītībā"*. 2021. gada 15. Oktobrī, Rīga, pp. 82–84, ISBN 978-9934-22-672-4

7. **Žentiņš, V**., Soročins, A., Koģenerācijas staciju ražošanas lēmumu pieņemšanas algoritms darbībā ar siltuma akumulatoru. *RTU 62. studentu zinātniski tehniskā konference. Sekcija "Ražošanas tehnoloģija"*. Rīga: RTU Izdevniecība, 2021, ISBN 978-9934-22-649-6

8. **Zentins, V**., Sorocins, A., Nagla, J., Rusovs, D., Insulation cost impact on heat accumulation unit heat loss. *RTU 61st International Scientific Conference.* 14 October 2020, ISBN 978-9934-22-503-1

9. **Žentiņš, V**., Valpētris, M., Ķibilds, A., Mitruma un temperatūras sensoru izstrāde. *RTU 59th International Scientific Conferenceconference,* Riga, 12 October 2018.

10. **Žentiņš, V**., Nagla, J. Ūdenssildāmā katla KVGM 100 efektivitātes paaugstināšana, izmantojot siltumsūkni. *RTU 59th International Scientific Conference,* Riga, 12 October 2018.

11. Nagla, J., **Žentiņš, V.**, Jaundālders, S., Soročins, A. Metodika tirgus apstākļiem piemērota centralizētās siltumapgādes sistēmas optimizācijas modeļa izstrādei, Latvija. *RTU 59th International Scientific Conference,* Riga, 12 October 2018.

Publications in scientific journals

1. Rusovs, D., Jakovļeva, L., **Žentiņš, V.**, Baltputnis, K. Heat Load Numerical Prediction for District Heating System Operational Control. *Latvian Journal of Physics and Technical Sciences*. 2021, Vol. 58, No. 3, pp. 121–136. ISSN 0868-8257

2. **Žentiņš, V.**, Rusovs, D., Soročins, A., Decision Making Control Algorithm for Cogeneration Plants in Operating with the Heat Accumulator Deep Analysis Model. Complex Systems Informatics and Modeling Quarterly Journal, 2022, Riga No. 30, ISSN: 2255-9922

1. LITERATURE REVIEW

1.1. Climate characteristics and possibilities to increase the efficiency of cogeneration plants

Latvia is located in the temperate climate zone, where summer and winter air temperatures are not only very seasonally variable, but also often change during the day, even in the 15–20 ºC range [7].

In order to ensure a stable heat load, it is necessary to continuously regulate the capacity of heat sources in a district heating system with changing climatic data. By producing in cogeneration mode, not only the heat load but also fluctuating electricity market prices, such as in the Nordpool system, are variable.

Heat accumulation makes it possible to separate the production of heat and electricity. In the conditions of the free heat energy market, accumulation provides an opportunity to flexibly follow the energy demand and to produce energy with the most efficient modes of the plant. This makes it possible to make efficient use of existing plant capacity, including peak-load electricity generation at a high market price. Thermal storage is 100 times cheaper than investing per unit of storage capacity for electricity [9].

In heat energy, heat storage accumulation with stratification is most often used, where both hot and cold water are stratified and are located in the reservoir at the same time. This decomposition occurs under the influence of Archimedes power [13]. This type of heat storage is the simplest and cheapest [12].

As technology advances, efficiency measures are gradually being introduced to increase the overall efficiency of the cogeneration plant. One of the current technologies is low-potential heat recovery from both flue gases and condensate.

1.2. Review of cogeneration plants in Latvia and production decision making

The liberalization of the energy market and the EU's targets for improving energy efficiency in each Member State [4] are contributing to the rapid development of heat accumulation facilities. Accurate production planning is very important in cogeneration plants operating in the free electricity market [40], [53], besides the use of heat accumulators increases significantly in terms of both complexity and additional calculation functions. In addition, the production process is affected by variable heat, CO_2 and fuel costs [41]. In Latvia, 175 stations produce 75 % of heat in cogeneration mode. In 2019, out of the total number of all CHPs, 159 received mandatory purchase (MP) support for electricity production. But the 5 largest stations with a capacity of more than 10 MWel received payment for installed capacity, which is the mandatory procurement component (MPC) from electricity for consumers. CHPs with a capacity of less than 10 MWel, that have received (MP) support, have a total installed electrical capacity of 199.2 MWel.

Number and total capacity of cogenerations
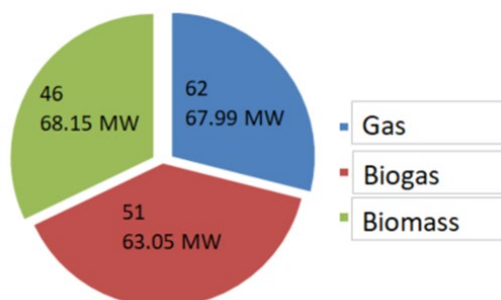
Fig. 1.2.1. Distribution of cogeneration units by fuel [42].

The total installed capacity of gas – 62, biogas – 51, and biomas – 48, CHP ranges from 63.05 MWel for biogas to 68.15 MWel for biomass. In turn, the installed capacity of the 5 largest electricity CHP receives 1061.90 MW of the installed capacity, which is also included in the MPC [4]. A total of 61 stations [43] out of 164 stations, or 37 % of the total share, will lose support from 2020–2022. Also, after 2022, the number of stations, which receive state aid, will decrease, as the guaranteed OI for electricity was provided for a support period of 10–15 years [44]. As a large number of CHP approaches or ends MPC support, it is necesaary to refocus on free market conditions, which means that electricity is not purchased at a guaranteed price rate.

In order to be able to accept the most accurate result for participation in the free electricity market in the shortest possible period (for example, the Nord Pool daily market, where supply and demand bids for the next day must be placed no later than at 12:00 on the current day) [22], during this period, it is necessary to be able to process a large amount of data. Such data volume contains the next day's heat load forecasts, the operation of the CHP, changes in the price of electricity, and, in the case of HS, its performance parameters. At this point, if not all circumstances are taken into account, there may be a case where CHP's operation with HS may not produce the maximum best result, or even a loss.

With changing external factors, such as heat load, as well as the market price of electricity [28], it is almost impossible to achieve perfect planning of cogeneration regimes for the next day, but this goal can be approximated by using different methodologies. There are several ways to achieve more flexible operation of cogeneration plants under market conditions [58], one of which is the use of heat accumulator [59]. In addition, planning the coherent operation of a cogeneration unit with HS can increase efficiency but complicates the planning task [60]. The aim of a cogeneration plant with multi-level heat storage control is to obtain the maximum positive result by quickly excluding those operating scenarios in which the operation of CHP with HS is not technically or economically feasible.
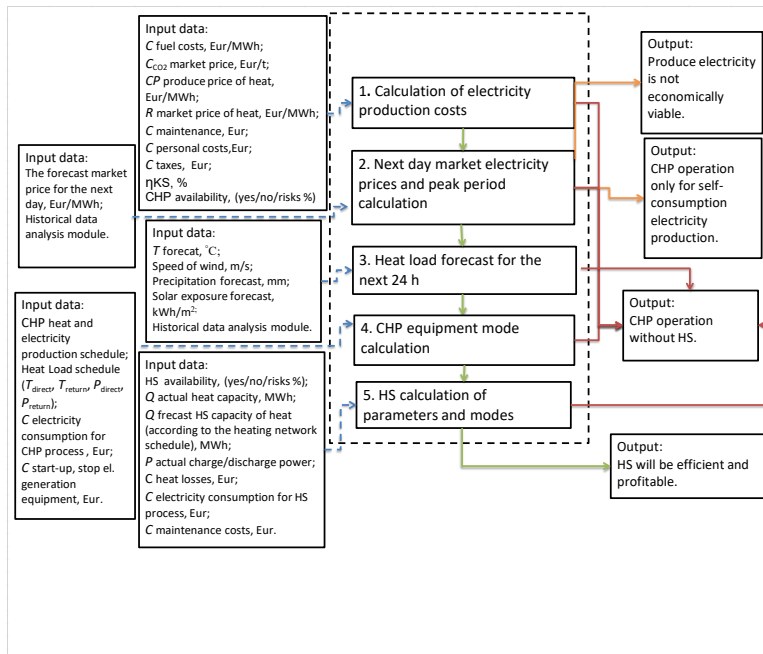
Fig. 1.2.2. Functional scheme for defining 5 variable blocks [62].

This algorithm consists of a multi-level system with the main 5 block calculation modules, which have their own input data, but each of them can interact with each other with its own function output or result. When all functions are exited, the cases of CHP operation with HS are filtered out, defining if they are effective or not. In addition, it is possible that by entering the input data in one of these blocks, the result shows that the use of HS is not useful.

In order to achieve the most efficient result, it is necessary to optimize a decision-making algorithm, it is necessary to combine these separate processes into a single one. The developed algorithm consists of 5 large basic block modules, which defines the main processes attaching great importance to the parameters and losses of the heat accumulator operating modes.

1. **Electricity first cost calculation model.** One of the key indicators for starting into a free market is accurate calculation of the current first cost of produced electricity [61], which is influenced by such variable factors as fuel costs, the cost of heat production against the selling price, as well as the CO_2 emission stock market factor if the plant does not use renewable fuels. In addition, the availability of equipment and operational risks are determined in this block.

2. **The electricity calculation module** determines the next day's electricity price forecasts. In the market price calculation, the maximum and minimum average price periods of electricity are analyzed and searched for and compared with the average cost price of electricity. In addition, many studies use analysis of historical data to help plan for a longer period of time [45].

3. **The heat load calculation module** provides an accurate heat load forecast for each hour [36] 24 hours ahead, which significantly affects the entire production planning process. As a result of an inaccurate forecast, the heat accumulator may be precharged prematurely, and by continuing production, it would no longer be possible to store excess heat, which would affect the possibility to reduce production capacity. Or there may be a situation where HS has not yet been discharged at the start of the new stock exchange cycle. Again, production cannot take place at the declared capacity.

4. **Cogeneration operating mode** is a technical one in which, depending on the ratio of heat and electricity energy and the flexibility of the generation blocks, a calculation has to be made in order to decide on the start of production. In addition, the start-up and shut-down conditions of the cogeneration unit and the range of production capacity during the day must be taken into account, which may damage the technical components of the plant [39]. In addition, the conditions and costs of starting and stopping the CHP installation must be taken into account [46].

5. **The heat accumulator calculation module** is the technical parameters of heat accumulation such as heat capacity, charging and discharging capacity, heat loss, electrical and other technical parameters. The availability of equipment for the accumulation system is very important.

1.3. Conclusions of Chapter 1

The analysis of the literature shows that in order to ensure a stable heat load, it is necessary to continuously regulate the capacity of heat sources in a district heating system with changing climatic data. In the operating conditions of the state MP support of cogeneration plants, the changing daily heat load affects the operating modes, but the production planning is relatively simple. With the loss of MP support, cogeneration modes are also affected by the volatile electricity market. As a result of many variables, it is difficult to make a production decision if it has to be made the next day, which must be done in the free market of electricity from 10:00–12:00 on this day, where demand and supply are created on the exchange. In addition, the use of heat storage and heat pump technology further increases uncertainty, as the technical and economic parameters of the equipment also need to be planned under changing market and environmental conditions.

For example, heat accumulator technology can increase the efficiency of a heat source but without planning and technological calculations can reduce efficiency or cause losses.

Five large basic blocks, which influence the cogeneration plant production decisions most, were defined for the algorithm – electricity costs, electricity market prices, heat load, cogeneration operation mode, and heat accumulator calculation modules. Each of the modules forms calculation processes, where the input data and equations form output functions with five states that define an economically sound production decision.

2. INCREASING OF HEAT SOURCE WORKING EFFICIENCY AND REDUCING OF EMISSIONS

2.1. Use of an absorption type heat pump

The use of a flue gas condenser is becoming a common solution to increase the efficiency of the plant. As a result, the overall efficiency of the system exceeds 100 % compared only to the efficiency of the boiler alone. The dew point of the boiler flue gas is about 50–60 ºC, which corresponds to the effective flue gas recuperation threshold and depends on the return temperature of the water of the DHS. Deep cooling of the flue gas (below 40–45 ºC) and recovery of the low potential is not possible with direct heat exchange between the flues and the return water of the network.

This chapter discusses the modernization of the existing flue gas condenser system, where an existing absorption type heat pump (AHP) with a nominal capacity of 2.1 MW was connected to recover additional heat from the flue gas. As a result of deep cooling of the flue gases, fuel consumption reduces which ensures reduced carbon emissions. The moisture content of the fuel and the hydrogen as a component create a significant concentration of moisture in the condensing flues. Exhaust moisture condensation increases combustion efficiency and reduces the level of emissions per unit of energy. For example, the combustion of methane produces a reaction product of at least 2.25 kilograms of water vapor per kilogram of methane. As a result of condensation, the amount of steam returns to the energy balance from 4 to 5 MJ per kilogram of fuel.

The return temperature values of the heating heat load modes determine the condensation rate and heat recovery. Figure 2.1.1 shows the coherence between condensation rates and heat recovery from the flue gas temperature [14]. The picture shows that only half of all possible moisture is condensed at 45 ºC.
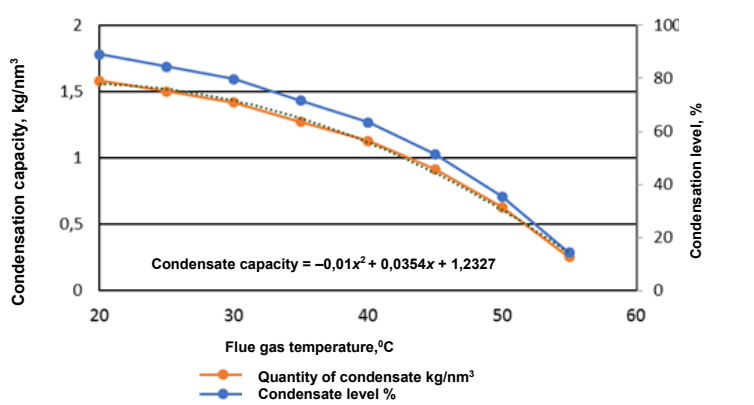
Fig. 2.1.1. Latent heat recovery from flue gases after natural gas combustion [14].

Lowering the flue gas temperature to 25–35 ºC allows the fuel efficiency of the gas boiler to be improved by up to 16 % [15] and the solid particles to be reduced by 33–44 % for biomass boilers [16]. Experimental results for fuels with a moisture content of 50.9 % show that using AHP will recover up to 44 % of energy from flue gases, compared to 23 % with FGC alone.

If district heating system uses AHP system, then very important is the quantity of heat supplied by the coefficient of performance (COP) Q_{sup} and Q_{rec} latent heat that is gained from flue gas ratio [17].

$$COP = \frac{Q_{sup}}{Q_{sup} - Q_{rec}}$$

(2.1.1)

Literature suggests that the COP of such systems at values of similar parameters can reach 1.762 [18]. The absorption system consists of three main parts: an absorber, in which the flue gases are cooled, a generator and a cooler, where the steam is evaporated and condenses at a higher pressure. The nominal cooling capacity is 2.1 MW, the water flow for cooling is 70 m^3/h and the flue gas cooling temperature is from 55 ℃ to 29 ℃. The heat supplied to the AHP consists of energy Q_{dr} (from hot flue gas, steam or water) which enters the generator with a nominal capacity of 2.7 MW. The nominal cooling performance is with a COP = 0.78 at a water circulation of 110 m^3/h in a closed circuit between FGC and AHP. Thus, the temperature in FGC is from T_{1C} = 17 ℃ to T_{2C} = 25 ℃. The amount of flue gas (Q_{rec}) or latent energy obtained in the FGC is used in the AHP evaporation process. The evaporated water is then absorbed by the Li-Br solution with energy. The return water flow to the DHN is limited and at the time of its observation is about 350 m^3/h. After heating into the absorber, this flow enters the AHP condenser, where energy of the steam generator (Q_{dr}) must be balanced by the return DHN flow. The return water flow obtains energy Q_{rec} in the absorber and Q_{dr} in the condenser. The total energy $Q_{sup} = Q_{dr} + Q_{rec}$ at temperature T_{2sup} is supplied to the DHN return water flow.

The aim of the study is to develop an empirical coherence between the heat recovery rate of different boilers with AHP and FGC operating modes. In real heating mode, the speed of power demand requires careful consideration of the effects of thermal inertia of the networks [19] and the market demand for energy storage charging planning [20]. The data shown in Figs. 2.1.3–2.1.5 were obtained after temperature and flow rate measurements at the given points according to the hourly operating period with the level of industrial accuracy.
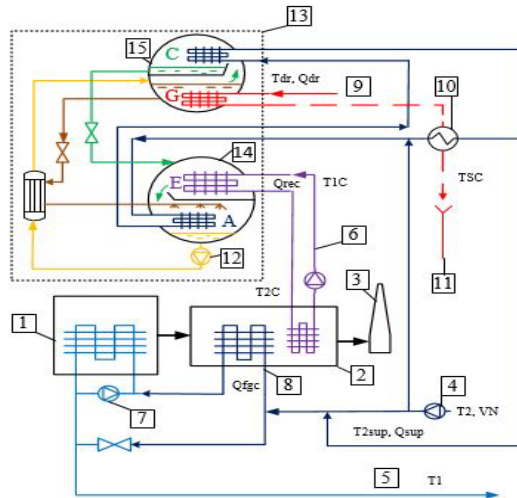
Fig. 2.1.2. Operation of an absorption heat pump and flue gas condenser for energy recovery: 1 – boiler ; 2 – flue gas condenser (FGC); 3 – chimney; 4 – network circulation pump, return water from the district heating network (DHN); 5 – direct water to DHN; 6 – flue gas energy condensation loop for AHP evaporator (E); 7 – boiler recirculation pump; 8 – flue gas energy loop; 9 – water steam supply to AHP; 10 – water vapor condenser cooler; 11 – water vapor condensate drain; 12 – LiBr solution circulation pump; 13 – absorption type heat pump (AHP); 14 – evaporator (E) and absorber (A); 15 – condensator (C) and generator (G) [21].

The dispersion of power and COP in the considered diagrams occurs over a wide range of operating parameters. For example, boiler output and return temperature T_2. The AHP capacity Q_{sup} values for the rated boiler capacity can be determined by evaluating the ATS performance. Heat recovery from steam condensate is provided in condenser cooling point No.10.

The significant AHP COP fluctuations for the change in boiler capacity can be explained by the different return temperature T2 values and the amount of water flow change in Q_{DR}. The trends in Fig. 2.1.3 show that the COP increases as the amount of flue gas increases with the amount of water vapor. AHP steam power Q_{DR} provides low potential heat recovery from flue gas cooling.
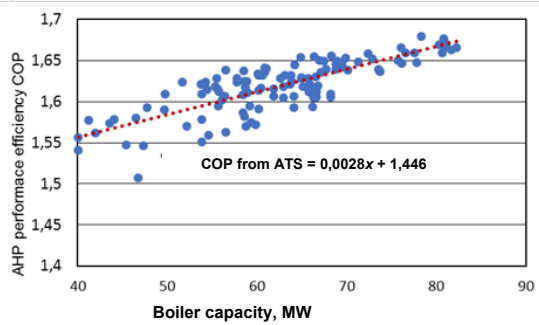
Fig. 2.1.3. Absorption type heat pump COP for different boiler capacities [21].

Figure 2.1.4 shows the coherence for energy recovery in FGC as a whole. It can be seen that the total energy recovery follows the increase in boiler capacity to a deviation where 5.2 MW of heat is recovered at 40 MW. At 80MW, the boiler capacity should be 10.4 MW, but in real operation the recovery value is only 9.5 MW.
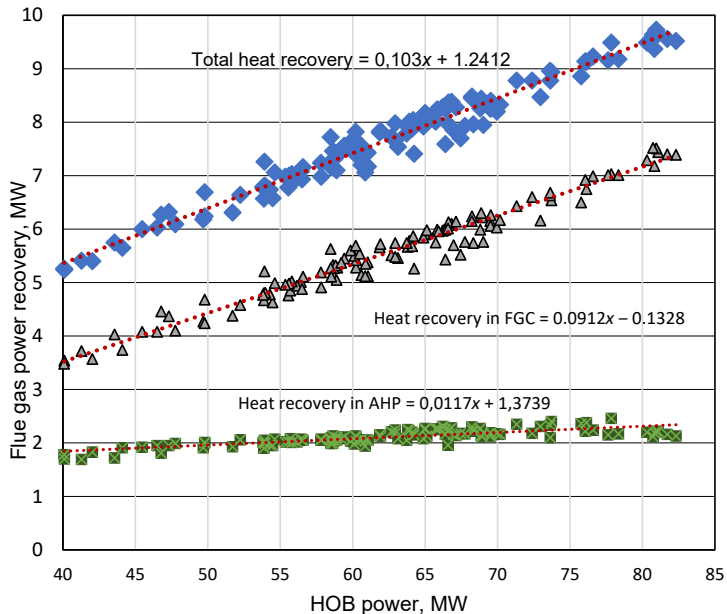
Fig. 2.1.4. Energy recovery from flue gases: AHP (Q_{rec}) ■, FGS (Q_{fgc}) ▲ and total ($Q_{rec} + Q_{fgc}$) ◆ [21].

This 10 % deficit can be explained by the limited Q_{rec}. When the boiler capacity doubles from 40 MW to 80 MW, the Q_{rec} value in the AHP system increases by 35–40 %. Empirical equations shown in the diagrams in Figs. 2.1.3 and 2.1.4, show the effect of the boiler on the capacity, return temperature T_2 and on the regeneration efficiency COP values. These relation coherences will open up road for production planning, simulation of heating network operation, as well as for further improvement of system operation.

2.2. Use of heat accumulator

Based on heat meter data for three yearly periods: 2015/2016, 2016/2017, and 2017/2018, the hourly data of KM heat load dynamics were analyzed. When performing data processing and constructing the heat load schedule, in Fig. 2.2.1 one can see the total heat source load in KM and CHP modes. As a result of modulation, a heat load schedule was compiled for CHP operation with HS.
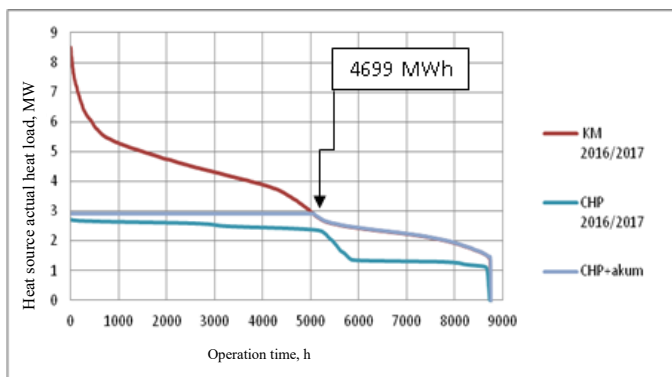
Fig. 2.2.1. KM heat load graph (for yearly period 2016/2017) [22].

For each heating period, the actual heat load duration schedule or the so-called Rosander schedule was compiled, dividing the cogeneration and boiler heat load separately (Fig. 2.2.1). The cogeneration unit is not in the maximum load section from ~ 4000 to 8760 hours.

To ensure the smooth operation of CHP in the market of variable heat load and electricity, there is a solution with the application of HS as shown in [23] Fig. 2.2.2. The figure shows that the main benefit from the application of HS are the smooth operation of the equipment and maximal use of cogeneration equipment in the peak hours of electricity prices. Modulating the situation to assess the operation of CHP with HS and possible additional electricity production comparing CHP without HS, Nordpool spot data was used, where it was possible to find hourly historical data on electricity prices in Latvia [8]. The calculations analyzed the difference in electricity prices between the average price during the "peak" period and the period when the electricity price has fallen (weighted average time outside the peak).
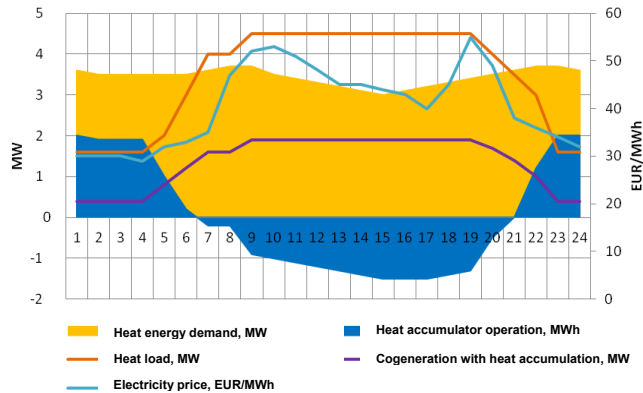
Fig. 2.2.2. Operation of a heat source with a heat accumulator for a 24-hour cycle [22].

By installing the HS, continuous operation of the cogeneration unit in the range from 50 % to 100 % of the installed capacity is achieved. Compared to the 3-year average heating period, it is possible to produce an additional 4,272 MWh of electricity in cogeneration mode and achieve 4,699 MWh of combined cycle heat energy.

Table 2.2.1

CHP Operation with and without Accumulator [22]

Combined heat and power	unit	Before 3-y average	After Forecast	Difference After-before
Electricity sold	MWh	14651	18453	3802
Heat energy sold	MWh	22061	22061	0
Electricity production in cogeneration mode	MWh	16462	20734	4272
Heat energy production	MWh	31516	31516	0
CHP	MWh	18108	22807	4699
Boiler	MWh	13408	8709	−4699
Fuel consumption	MWh	54836	60721	5885
CHP	MWh	41155	51834	10680
Boiler	MWh	13682	8887	−4795

By generating more electricity at the existing heat load and contributing to the longer operation of the cogeneration unit, which is more efficient, fuel savings and reductions in CO_2 emissions of around 959 tonnes are achieved [24], if compared to the amount of heat produced to balance gas boilers. The results of the study are summarized in Table 2.2.1 and show that the fuel economy of this plant is comparable to 4795 MWh.

2.3. Cnclusions of Chapter 2

1. Increased efficiency, reduced emissions and balanced heat loads can be achieved by upgrading plants with heat storage and heat pump technology during the operational phase.

Deep flue gas cooling with an absorption heat pump has a wide range of applications: cogeneration and water heating boilers to improve efficiency. There are many components of efficient energy recovery from flue gases (flue gas condensers, absorption coolers, heat exchangers, etc.). There are still not enough studies to determine the rated capacity of a heat pump for different operating conditions. Experimental and theoretical calculation data show that the thermal efficiency of the boiler can be improved by up to 16 % if the flue gas temperature is reduced to 25 ºC.

2. Analysis of real data shows that electricity prices at night are often lower, but at this point the heat load increases, while during the day hours at lower heat load electricity prices reach their peaks. Temporary heat accumulation allows to balance the heat load and accumulate additional heat during the day. The study shows that the use of heat storage equipment in a cogeneration plant with cogeneration units with a total electrical capacity of 2.64 Mwel enables the production and sale of up to 4272 MWh of additional electricity per year at the existing heat load. In the case of fossil fuels, 959 t CO_2 emissions are saved.

3. METHODOLOGY FOR CALCULATING HEAT LOSS IN ACCUMULATOR OPERATION MODE

In Europe, heat accumulation facilities are more common in the Nordic countries, with Denmark and Sweden leading the way. The total heat capacity of accumulation tanks is high, for example, 42 GWh in Sweden and even 50 GWh in Denmark. Denmark has the largest heat accumulation tanks in Europe. The largest tank is currently in Odense, with a capacity of 75,000 m^3 and able to reach a heat capacity of 3.6 GWh [12].

In Latvia, the first big size heat accumulators with a volume of over 1000 m^3 were built starting in year 2019, when the first one – "Salaspils Siltums" Ltd – with a volume of 8000 m^3 was opened. In the same year, in the city of Jelgava, the "Fortum Latvia" Ltd built a HS of 5000 m^3 with a heat capacity 180 MWh [26]. "Latvenergo" CHP-2 was put into operation on March 26, 2021 and is the largest HS in the Baltics, with a volume of 18,000 m^3, which is comparable to the Nordic HS.

The thickness of the thermal insulation and the thermal conductivity of HS affect not only the losses but also the efficiency. Poor thermal insulation causing large heat losses can disrupt stratification within HS and hot and cold water layers [55], [56]. The efficiency is also influenced by the form of HS, where stratification becomes more pronounced in case of higher height-to-diameter ratio [57]. The main goal of this chapter is to determine the efficiency of the thermal insulation solution of three real heat accumulators and to perform their analysis, which is used for 3 largest heat accumulators in Latvia. Heat transfer calculations will be performed for stationary mode, and modeling will be performed at the HS charge-discharge cycle.

Coefficient U is the main parameter which is used to determine the thermal insulation. Coefficient U depends on the thermal resistance:

$$U = \frac{1}{R} = \frac{1}{\frac{\delta_1}{\lambda_1} + \frac{\delta_2}{\lambda_3} + \frac{\delta_n}{\lambda_n}}, \text{ W/(m}^2\cdot\text{K)}, \tag{3.1}$$

where R is thermal resistence; δ is layer thickness of the material, m; and λ is coefficient of thermal conductivity of materials, W(m·K) [29].

The calculation will be performed in a HS with a volume of $V = 5000$ m^3 and the same geometric dimensions – $S_{bas} = 200.96$ m^2, $S_{roof} = 220$ m^2, $S_{walls} = 1246$ m^2, but the thermal insulation solution will differ from data in Table 3.1 as in objects x, y, and z. When calculating heat losses at 0 °C air temperature, 75 °C for hot layer, 47 °C for cold layer, which corresponds to a real DHN graph. The temperature of the mixing zone is thus assumed to be 60 °C. Typical dimensions are: the heat accumulator height – 25.86 m and a diameter – 16 m. In order to obtain a more reliable result for the simulation, the α values at the selected heat accumulator performance parameters for both forced and free convection will be determined.

Determining or modeling theoretical heat loss in HS required extensive calculations performed by the author in Microsoft Excel computer program. In order to be able to perform modeling for thermal insulation solutions, a calculation methodology in the form of a block diagram was developed, which is shown in Fig. 3.1.

Insulation Solutions for the Largest Heat Accumulators in Latvia [30]

Name of the heat storage construction	Layer	Object, material	Thickness, m	λ, W/(m·K)	Object, material	Thickness, m	λ, W/(m·K)	Object, material	Thickness, m	λ, W/(m·K)
		Object x			Object z			Object y		
Roof	1	Steel	0.006	50	Steel	0.006	50	Steel S355 J2H	0.006	50
	2	Paint (polyurethane base)	0.0002	0.2	Paint (polyurethnane base)	0.0002	0.2	Paint (polyurethnane base)	0.0002	0.2
	3	*Ro*kwool sl960	0.5	0.045	*PAROC ROS 30*	0.26	0.036	*PAROC ROS 30*	0.3	0.036
	4	External steel	0.0006	14.4	*PAROC ROS 50*	0.04	0.038	*PAROC ROB 80*	0.02	0.038
	5				External steel	0.0006	14.4	External steel	0.0006	14.4
		U, W/(m²·K)	**0.0899**				**0.1208**			**0.11285**
Walls	1	Steel	0.18	50	Steel	0.012	50	Steel S355 J2H	0.08	50
	2	Paint (polyurethane base)	0.002	0.2	Paint (polyurethnane base)	0.002	0.2	Paint (polyurethnane base)	0.002	0.2
	3	*Rokwool sl930*	0.4	0.049	*PAROC WAS 50*	0.3	0.034	*PAROC ROS 30*	0.3	0.036
	4	External steel	0.0006	14.4	External steel	0.0006	14.4	*PAROC WAB 10t*	0.02	0.036
	5							External steel	0.0006	14.4
		U, W/(m²·K)	**0.12233**				**0.1132**			**0.11235**

The calculation will be performed in a HS with a volume of $V = 5000$ m³ and the same geometric dimensions – $S_{bas} = 200.96$ m², $S_{roof} = 220$ m², $S_{walls} = 1246$ m², but the thermal insulation solution will differ from data in Table 3.1 as in objects x, y, and z. When calculating heat losses at 0 °C air temperature, 75 ºC for hot layer, 47 ºC for cold layer, which corresponds to a real DHN graph. The temperature of the mixing zone is thus assumed to be 60 ºC. Typical dimensions are: the heat accumulator height – 25.86 m and a diameter – 16 m. In order to obtain a more reliable result for the simulation, the α values at the selected heat accumulator performance parameters for both forced and free convection will be determined.

Determining or modeling theoretical heat loss in HS required extensive calculations performed by the author in Microsoft Excel computer program. In order to be able to perform modeling for thermal insulation solutions, a calculation methodology in the form of a block diagram was developed, which is shown in Fig. 3.1.

Input data:
Heat storage δ – material layer thickness, m;
λ – coefficient of thermal conductivity of materials, W/(m·K);
Outside temperature $T_{outside}$;
Wind speed $v_{wind\,speed}$, m/s;
Water temperature in HS T_v.

1

Thermal insulation resistance of a heat accumulator determined by coefficient U:

$U_0 = 1/R_0$,

$R_0 = R_{ins} + R_1 + R_2 + R_n + R_{out} = \frac{1}{\alpha_{ins}} + \frac{\delta_1}{\lambda_1} + \frac{\delta_2}{\lambda_2} + \frac{\delta_n}{\lambda_n} + \frac{1}{\alpha_{out}}$,

where R – thermal resistance; δ – material layer thickness, m;
λ – coefficient of thermal conductivity of materials, W(m·K);
α – heat transfer coefficient, W/(m²·K).

Calculate the Grashof number:

$Gr = \frac{g \times l^3 \times \beta \times \Delta t}{v^2}$, m/s²;

where g – acceleration of free fall (9,81 m/s²), m/s²; l – characteristic size, m; β – coefficient of thermal expansion of the volume, 1/K;
Δt – the difference between the ambient and wall temperature, °C;
v – kinematic viscosity of the environment, m²/s.

2

The heat transfer coefficient α is formed by free and forced convection.
Free convection is on both the inner (water) and outer surfaces (air). Forced convection on the outer surface where the wind acts.

Calculation of free convection

Calculation of the horizontal surface-roof:
The average convective heat transfer coefficient $\bar{\alpha}$ is determined by the formula $\bar{\alpha} = (\overline{Nu} \times \lambda)/l$, where $\overline{Nu}$ – the average number of Nuselt; l – characteristic size, m.

Calculation of vertical surface - walls:
$\bar{\alpha} = \bar{\alpha}_l \frac{h_x}{h} + \bar{\alpha}_t \left(1 - \frac{h_x}{h}\right)$, where $\bar{\alpha}_l$ – average value of heat transfer coefficient for the lower part of the surface (laminar mode); $\bar{\alpha}_t$ – average value of heat transfer coefficient for the upper part of the surface (turbulent mode).

Calculation of forced convection

Forced convection is calculated for the outer surfaces:

$\bar{\alpha}_{out} = \frac{\lambda \overline{Nu}_l}{l}$.

The formula used to calculate for any surface shape in the case of free convection.

$\overline{Nu} = C \times (Gr Pr)^n$,

where C and n – coefficients depending on the flow mode; Gr – Grashof number; Pr – Rrandtl number.

Laminar layer height h_x

$Gr Pr = \frac{g \times h_x^3 \times \beta \times \Delta t}{v^2} Pr > 10^9$

Find the height h_x of the laminar layer: $h_x = \sqrt[3]{\frac{10^9 v^2}{g \beta \times \Delta t Pr}}$.

At the bottom of the height along the surface is a laminar flow found by the formula:

$\overline{Nu}_l = 0{,}535(Gr_l Pr_s)^{0{,}25}$.

There $(Gr Pr_s) = 10^9$, because such a condition was calculated hx (the laminar mode switches to turbulence).

Flow mode:
$\overline{Nu}_t = 0{,}15(Gr_l Pr_s)^{0{,}33}$.

$\overline{Nu} = C Re^{0{,}8} Pr_s^{\,0{,}43} (Pr_s/(Pr_v))^{0{,}25}$

$Re = \frac{\omega \times l}{v}$,

where ω – average wind speed, m/s.

Laminar boundary-layer flow:
$\bar{\alpha}_l = \frac{\lambda \overline{Nu}_l}{h_x}$.

Turbulent boundary-layer flow:
$\bar{\alpha}_t = \frac{\lambda \overline{Nu}_t}{h}$.

3 Calculates heat loss for walls and roof:
$Q = S \times U_0 \times (t_{outside} - t_{inside})$,
where t_{v1} – ambient temperature, °C; t_{v2} – outside temperature, °C;
S – the surface area of the enclosing structure, m².

4 Heat loss through the foundation of the tank:
$Q = S \times U_p \times (t_{outside} - t_{inside})$.

5 Calculate the total heat loss:
$Q = Q_{foundation} + Q_{walls} + Q_{roof}$.

Calculate the heat transfer coefficient U_p for foundation

$U_p = \frac{2\lambda}{\pi B' + d_1} \ln(\frac{\pi B'}{d_1} + 1)$, where λ – ground thermal conductivity, W/m·K; B' – the characteristic size of the floor, m; d_1 – equivalent floor thickness, m.

Calculate the equivalent floor thickness
$d_1 = w + \lambda(R_{si} + R_f + R_{se})$,
where w – full foundation thickness, m; λ – thermal conductivity of unfrozen ground, W/(m·K); R_{si} – resistance to heat loss on the inner surface, m²K/W; R_f – heat loss resistance of the foundation, m²·K/W; R_{se} – external surface heat loss resistance, m²·K/W.

Calculated characteristic size of the floor
$B' = A/0{,}5P$, m
where A – area of foundation, m²; P – perimeter of foundation, m.

Fig. 3.1. Methodology of heat loss calculation [29], [31]–[33].

An important indicator of the efficiency of a heat accumulator is not only the calculation of heat loss, but also the height of the thermocline. The height of the thermal wedge in different operating modes can reduce or increase the heat capacity of the battery. Figure 3.2 shows that the height of the thermocline is influenced by such factors as the ratio of the height and diameter of the heat accumulator [57] and the thermal insulation efficiency [56].

Fig. 3.2. Example of thermal wedge of heat accumulator [63].

The height of the thermocline is calculated using differential equations.
The continuity equation expresses the mass of water in the charged battery over the cycle. It is expressed according to the coordinate system:

$$\frac{\partial \rho}{\partial t} + \rho\left[\frac{1}{r}\frac{\partial (rV_r)}{\partial r}\right] + \frac{1}{r}\frac{\partial V_\theta}{\partial \theta} + \frac{\partial V_z}{\partial z} = 0 \tag{3.2}$$
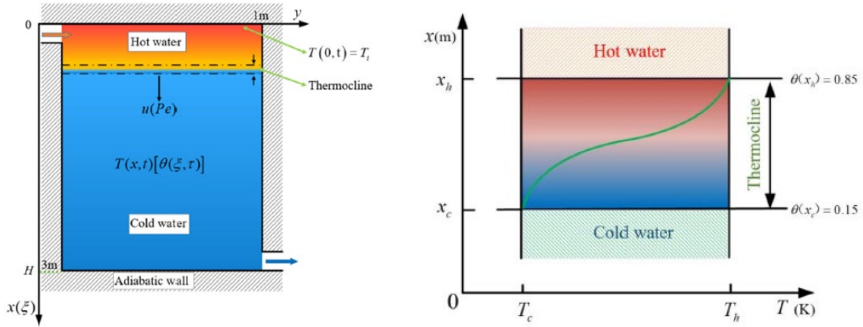
The impulse equation provides the development of the liquid flow rate in the storage tank (V_r, V_Θ, and V_z) and the pressure field. It is expressed on the r axis as in Eq. (3.2):

$$\rho\frac{\partial V_r}{\partial t} + \frac{1}{r}\frac{\partial (r\rho V_r V_r)}{\partial r} + \frac{\rho}{r}\frac{\partial (V_\theta V_r)}{\partial \theta} + \rho\frac{\partial (V_z V_r)}{\partial z}$$
$$= -\rho\frac{\partial P}{\partial r} + \mu\left[\frac{\partial}{\partial r}\left(\frac{1}{r}\frac{\partial (rV_r)}{r}\right)\right] + \mu\left[\frac{1}{r^2}\frac{\partial^2 V_r}{\partial \theta^2} + \frac{\partial^2 V_r}{\partial z^2}\right] + \mu\left[-\frac{2}{r^2}\frac{\partial V_\theta}{\partial \theta}\right] + \frac{\rho V_\theta^2}{r} + \rho g_r \beta \Delta T . \tag{3.3}$$

The impulse equation is expressed on the axis:

$$\rho\frac{\partial V_\theta}{\partial t} + \frac{\rho}{r}\frac{\partial (r\rho V_r V_\theta)}{\partial r} + \frac{\rho}{r}\frac{\partial (V_\theta V_\theta)}{\partial \theta} + \rho\frac{\partial (V_z V_\theta)}{\partial z} =$$
$$= -\frac{1}{r}\frac{\partial P}{\partial \theta} + \mu\left[\frac{\partial}{\partial r}\left(\frac{1}{r}\frac{\partial (rV)}{\partial r}\right)\right] + \mu\left(\frac{1}{r^2}\frac{\partial^2 V_\theta}{\partial \theta^2} + \frac{\partial^2 V_\theta}{\partial z^2}\right) + \mu\left(\frac{2}{r^2}\frac{\partial V_\theta}{\partial \theta}\right) - \frac{\rho V_r V_\theta}{r} + \rho g_\theta \beta \Delta. \tag{3.4}$$

Imulse equation expressed on the z axis:

$$\rho\frac{\partial V_z}{\partial t} + \frac{\rho}{r}\frac{\partial (r\rho V_r V_z)}{\partial r} + \frac{\rho}{r}\frac{\partial (V_\theta V_z)}{\partial \theta} + \rho\frac{\partial (V_z V_z)}{\partial z} = -\frac{\partial P}{\partial z} + \mu\left[\frac{\partial}{\partial r}\left(\frac{1}{r}\frac{\partial (rV_z)}{\partial r}\right)\right] + \mu\left(\frac{1}{r^2}\frac{\partial^2 V_z}{\partial \theta^2} + \frac{\partial^2 V_{\theta z}}{\partial z^2}\right) +$$
$$+ \rho g_z \beta \Delta T . \tag{3.5}$$

The energy equation is expressed as follows:

$$\rho C\frac{\partial T}{\partial t} + \rho C\overline{u}\, \nabla T = \nabla(\lambda \nabla T) . \tag{3.6}$$

The continuity equation is expressed in polar coordinates:

$$\frac{\partial U}{\partial r} + \frac{\partial V}{\partial z} + \frac{U}{r} = 0 \tag{3.7}$$

The impulse equation is projected on the r axis as in the following equation:

$$\frac{\partial U}{\partial t} + U\frac{\partial U}{\partial r} + V\frac{\partial U}{\partial z} = \frac{1}{\rho}f_r - \frac{1}{\rho}\frac{\partial P}{\partial r} + \vartheta\left(\frac{\partial^2 U}{\partial r^2} + \frac{1}{r}\frac{U}{r} - \frac{U}{r^2} + \frac{\partial^2 U}{\partial z^2}\right). \tag{3.8}$$

The impulse equation is projected on the z-axis as in Eq. (3.9):

$$\frac{\partial V}{\partial t} + U\frac{\partial U}{\partial r} + V\frac{\partial V}{\partial z} = \frac{1}{\rho}f_z - \frac{1}{\rho}\frac{\partial P}{\partial z} + \vartheta\left(\frac{\partial^2 V}{\partial r^2} + \frac{1}{r}\frac{V}{\partial r} - \frac{V}{r^2} + \frac{\partial^2 V}{\partial z^2}\right) \tag{3.9}$$

Heat transfer energy equation allows to calculate the temperature field:

$$\frac{\partial T}{\partial t} + U\frac{\partial T}{\partial r} + V\frac{\partial T}{\partial z} = \frac{\lambda}{\rho C_p}\left(\frac{\partial^2 T}{\partial r^2} + \frac{1}{r}\frac{\partial T}{\partial r} + \frac{T}{\partial z^2}\right). \tag{3.10}$$

The vortex equation is derived from (3.7) and (3.8). The first equation is differentiated with respect to z and the second is differentiated with respect to r, the second equation is also subtracted from the first:

$$\omega = \frac{\partial U}{\partial z} - \frac{\partial V}{\partial r}. \tag{3.11}$$

Thus, the vortex equation can be expressed:

$$\frac{\partial \omega}{\partial t} - \frac{U}{r}\omega + U\frac{\partial \omega}{\partial r} + V\frac{\partial \omega}{\partial z} = -\frac{1}{\rho}\left[\text{rot}\right]_{\emptyset} + v\left(\frac{\partial^2 \omega}{\partial r^2} + \frac{1}{r}\frac{\partial \omega}{\partial r} - \frac{\omega}{r^2} + \frac{\partial^2 \omega}{\partial z^2}\right), \tag{3.12}$$

where $F = [f_r f_z]$, an additional equation is needed because it is necessary to calculate U and V. The equation of the flow function ψ is obtained:

$$U = -\frac{1}{r}\frac{\partial \psi}{\partial z} \qquad V = \frac{1}{r}\frac{\partial \psi}{\partial r}. \tag{3.13}$$

Putting U and V into Eq. (3.11), the following equation is obtained:

$$\frac{\partial^2 \psi}{\partial r^2} - \frac{1}{r}\frac{\partial \psi}{\partial r} + \frac{\partial^2 \psi}{\partial z^2} = -r\omega. \tag{3.14}$$

The lifting forces due to the difference in density are expressed by the Boussines approximation:

$$\rho(T) = \beta\rho_0(T - T_0), \tag{3.15}$$

where β is coefficient of thermal expansion; g is acceleration of gravitation; and T_0 is temperature.

This equation is used to express the Boussines approximation in vortex transport:

$$\frac{1}{\rho_0}\left[\text{rot}f\right]_{\emptyset} = \frac{1}{\rho_0}\frac{\partial \rho(T)}{\partial x} = g\beta\frac{\partial T}{\partial x} \tag{3.16}$$

Continuity equation (in three dimensions):

$$\frac{\partial \rho}{\partial t} + \sum_{i=1}^{3}\frac{\partial}{\partial x_i}(\rho u_i) = 0. \tag{3.17}$$

Three-dimensional energy transfer equation:

$$\rho c \frac{\partial T}{\partial t} = \text{div}(\lambda \text{grad} T) + T\beta \frac{dP}{dt} - \frac{2}{3}\mu(\text{div}\vec{u})^2, \quad (3.18)$$

where β is coefficient of thermal expansion of the volume and μ is dynamic viscosity.

One-dimension energy transfer equation:

$$\rho c \frac{\partial T}{\partial t} + \rho c v \frac{\partial T}{\partial x} = \lambda \frac{\partial^2 T}{\partial x^2}. \quad (3.19)$$

Dimensionless temperature in volume in direction x:

$$\theta(x) = \frac{T(x) - T_C}{T_h - T_C}. \quad (3.20)$$

A thermocline occurs when the heat accumulator is charging and hot water is flowing in from above T_h. The thermocouple is formed due to the different densities of water that are affected by its temperature [63].

Thermocline exists when $0.15 < \theta(x) < 0.85$, upper side of thermal wedge is $\theta(x_h) = 0.85$ and bottom $\theta(x_c) = 0.15$.
The purpose is to determine the thickness of the thermal wedge $\Delta h = x_h - x_c$. Coordinates without dimensions ξ and time τ or Fourier number

$$\xi = \frac{x}{H} \quad \text{and} \quad \tau = \text{Fo} = \frac{t\,a}{H^2}, \quad (3.21)$$

where $a = \frac{\lambda}{c\rho}$ is temperature conductivity; H is height of container; and t is filling time.

Table 3.2

Limits of Conditions (depths – x, time – t)

	Temperature	Dimensionless temperature
Tank start temperature (cold condition)	$T(x,0) = T_C$	$\theta(\xi, 0) = 0$
Warm water charging (from above)	$T(0,t) = T_h$	$\theta(0, \tau) = 1$
Accepted temperature from outside	$T_c = T(\infty,0)$	$\theta(\infty, 0) = 0$

Dimensionless speed or Péclet **number**:

$$u = Pe = \frac{vH}{a}, \quad (3.22)$$

where $v = \frac{Q}{A}$, convective velocity for downward movement of the thermal wedge; A is cross-sectional area of the container; and Q is volume flow during charging m^3/s.

The following conditions are accepted to find an analytical solution:

- Thermal wedge temperature distribution is asymmetric and independent of radial distribution without mixing or interference.
- The heat loss caused by passing through the container wall is negligible.
- The inlet temperature and mass flow are kept constant.
- The thermal boundary conditions of the top and bottom cover and side surfaces are adiabatic.

Laplace's analytical solution is transformed:

$$\theta(\xi, \tau) = \frac{1}{2}\left[\operatorname{erfc}\left(\frac{\xi - u\tau}{2\sqrt{\tau}}\right) + e^{u\xi}\operatorname{erfc}(\frac{\xi + u\tau}{2\sqrt{\tau}})\right],$$

(3.23)

where erfc() is error function.

It can be simplified because x and t are both greater than 0, but the equation approaches 0:

$$\theta(\xi, \tau) = \frac{1}{2}\left[erfc\left(\frac{\xi - u\tau}{2\sqrt{\tau}}\right)\right].$$

(3.24)

One dimension cannot completely analytically solve the problem of temperature distribution, therefore, it is necessary to introduce correction through coefficient ε and normalized time $\bar{t} = Pe\ Fo$:

$$\theta(\xi, \tau) = \frac{1}{2}\left[\operatorname{erfc}\left(\frac{\xi - \bar{t}}{2\sqrt{\bar{t}}}\sqrt{Pe}\right)\right].$$

(3.25)

The Peclet number is expressed by formula

$$Pe = \frac{vH}{\varepsilon a}.$$

(3.26)

During experiments it has been found that [64]

$$\varepsilon = 1.22\ x\ 10^{-6}e^{2.29\ln(Re_s)},$$

(3.27)

where the Reynold's number of the tank

$$Re_s = \frac{vD}{v} < 1708.$$

(3.28)

Diffuser outlet (hot water)

$$Re_i = \frac{q}{v},$$

(3.29)

where q is the flow per unit length of the diffuser perimeter $q = Q/(\pi d)$ and q is the volume flow per unit length of the diffuser, which is the perimeter of the diffuser plate.

Fruda's number is

$$Fr_i = \frac{q}{\sqrt{(h^3 g\frac{\Delta\rho}{\rho})}},$$

(3.30)

where
ρ is water density in the containertank and Δρ is between the water in the tank and the water flowing in from the diffuserdensity difference-tank and diffuser inlets
Then the initial thickness of the thermocline is

$$\delta_0 = 5.74 Fr_i^{1.34} Re_i^{-0.48}.$$

(3.31)

Richardson number shows the mixing ratio that is widely used to estimate thermal stratification in a hot water storage tank [65]:

$$R_i \ = \ \frac{g\beta h(T_{top} - T_{bott})}{V_s^2} > 1,$$

$$(3.32)$$

where V_s is inlet velocity through the diffuser:

$$V_s \ = \ \frac{4Q}{\pi d^2}$$

$$(3.33.)$$

Influence of Richardson Number on Thermal Stratification [64]

$Ri < 3.6$	Inlet geometry has a significant effect on stratification
$Ri > 10$	The inlet effect can be ignored
$Ri > 10$–20	A clear mix is observed
$Ri = 0.615$	Stratification appears

Figure 3.3 shows operator control tool for control of heat accumulator operating parameters, where it can be established that the height of the thermal wedge is 1 m (in the area with the red dashed line). The thermal wedge formed at this point in the operating mode is located in the zone of 6.5 and 7.5 m.
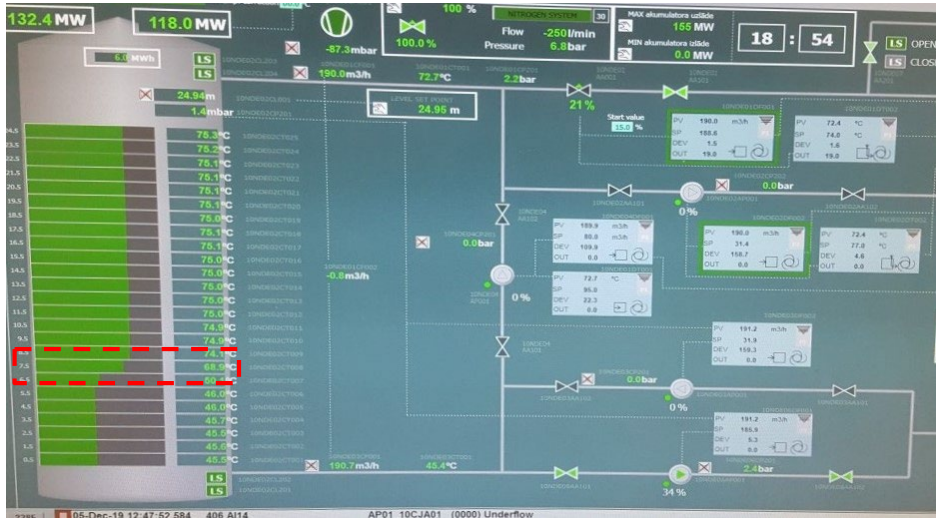
Fig. 3.3. Heat accumulator at the end of the charging cycle.

In Fig. 3.4, a heat loss calculation methodology for a heat accumulator has been developed, which is combined with both Fig. 3.1 calculation methodology and thermal wedge calculation. The basic calculation functions are defined in the flowchart in order to be able to find the heat loss for each hour, which is combined to obtain one operating cycle from charging to discharging.

Fig. 3.4. Flowchart showing the calculation of heat loss of the operating mode of a heat accumulator [62].
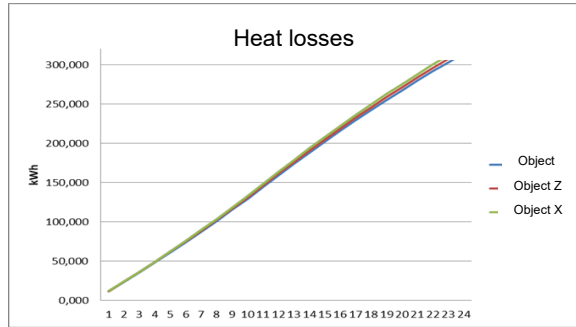

Fig. 3.4. Heat loss of HS for a period of 24 hours [29].

The lowest heat losses were for the thermal insulation solution of object Y with 314.29 kWh in the 24h period, which is by 2.8 % better than the thermal insulation solution of object X and by 1.4 % better than the thermal insulation solution of object Z. The research results show that the theoretical calculation and operation mode is very close to all 3 thermal insulation solutions, although a choice of different materials and thicknesses was used.

3.1. Conclusions of Chapter 3

Determining the theoretical heat loss for heat storage in operating modes requires extensive multi-step calculations, as many factors such as thermal insulation resistance, variable internal temperature changes, free and forced convection, outdoor temperature, wind and other factors must be taken into account.
The study showed that an important indicator of the efficiency of a heat accumulator is not only the calculation of heat loss, but also the height of the thermal wedge. In addition, the height of the thermal wedge affects heat loss in different operating modes but can reduce or increase the heat capacity of the battery. The height of the thermocline is influenced by such factors as the ratio of the height and diameter of the heat accumulator and the efficiency of thermal insulation.

A multi-stage heat loss and thermal wedge calculation methodology was developed to be able to integrate these equations as part of a module for in-depth analysis of a heat accumulator in a common cogeneration plant decision making algorithm.

When collecting data from the 3 largest heat accumulators in Latvia and their thermal insulation solutions, it was found that different solutions were used, including thickness. For example, the heat transfer coefficient U of the roof of object X with a thickness of 0.5 m is the best 0.089 W/m²·K, but for the walls it was the worst 0.122 W/m²·K. The different thermal insulation solutions in the calculations showed that the values of coefficient U are very close and in the modulation of the 24-hour operating mode at the same parameters, a difference of 2.8 % in heat loss was obtained between the objects. The lowest heat losses were for the thermal insulation solution of object Y with 314.29 kWh.

4. USE OF THE EXPERIMENTAL METHOD FOR THE DETERMINATION OF ACTUAL HEAT LOSS

Currently, one of the largest heat storage tanks in Latvia is located at the biomass cogeneration plant in Jelgava, Rupniecibas Street 73, which was put into operation on November 1, 2019. The responsible construction manager of this facility was the author of this Doctoral Thesis.

Fig. 4.1. Basic arsenal works of heat accumulator and assembly of metal structures (author's photo).

The thermal insulation of the accumulator is made of 300 mm thick PAROC ROS30 in 3 layers of 100 mm. Both the roof and the walls are additionally covered with extra hard 20 mm thick PAROC ROB80 and WAB10t for impact of thermal bridges and windproof. The main goal of the experiment was to determine the real heat loss of the HS under environmental conditions.

The experiment was an organized test that contained measurements for the cooling process of the HS tank from August 31, 2020 until September 7, 2020. During this period, the HS system was completely shut down and no technological activity such as the charging or discharging process, drainage or refilling took place. The average approximate temperature during the experimental period was +17.09 ºC, the average wind speed was 3.14 m/s. Uncontrollable factors that were not taken into account were humidity and exposure to sunlight. An observation period was chosen in which no precipitation was observed that would lead to an additional pssibility of error. During this period, a decrease in the HS water temperature was observed at 25 points throughout its height.
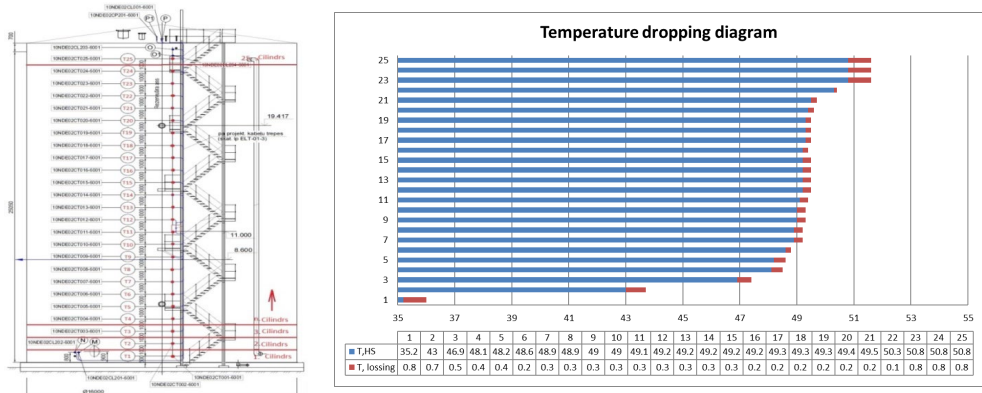

Fig. 4.2. Location of heat accumulator temperature sensors and temperature drops [62].

Figure 4.2 shows the location of temperature sensors from T1 to T25 on the tank. To determine the actual heat losses under real environmental conditions, the HS was divided into 25 separate layers or cylinders with their own volume or zones where temperature sensors with a certain volume are located.

The heat losses for each individual layer with volume were determined using the formula:

$$Q_{sl} = V_{sl} \cdot \rho \cdot c_p \cdot dT \qquad (4.1)$$

where T_1 is starting temperature, °C; T_2 is final temperature °C; and V is water volume in the measuring zone, m³ [29].

The total heat losses are obtained by summarizing heat losses of each layer:

$$Q = Q_{sl.1} + Q_{sl.2} + Q_{sl.n} + Q_{sl.25} \qquad (4.2)$$

	1	2	3	4	5	6	7	8	9	10	11	12	13	14	15	16	17	18	19	20	21	22	23	24	25
Lossing kwh	184.3	161.3	115.2	92.19	92.19	46.09	69.14	69.14	69.14	69.14	69.14	69.14	69.14	69.14	69.14	46.09	46.09	46.09	46.09	46.09	46.09	23.05	184.3	184.3	184.3
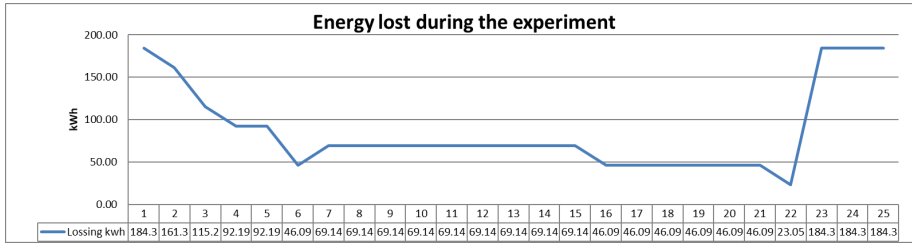
Fig. 4.3. Het loss profile for the accumulator [62].

The obtained results in Fig. 4.3 show HS in 7 days, or 168 h temperature drops. The largest drops were indicated by the tank temperature sensor No. 1 and the upper ones by Nos. 23, 24, and 25 by the maximum temperature drop of 0.8 ºC. In turn, in the middle part of the tank, sensors No. 16–22 showed a temperature drop from 0.1 to 0.2 ºC.

The largest heat losses occur in cylinders 1, 23, 24, 25, each of which accounts for 184.4 kWh. These 4 measuring heat losses account for 34 % of all heat losses. The total heat losses during this observation period make 2160.46 kWh or power 12.71kW.

4.1. Verification of heat accumulator's heat loss

The obtained data allow to evaluate the accuracy of the calculation against real experimental values and to introduce a correction coefficient. This method makes it possible to determine the effect of total thermal bridges on the structure. As shown in Fig. 4.1.1, the thermal bridges cover the entire tank of both the roof and the walls and also the foundation after the battery has been handed over.
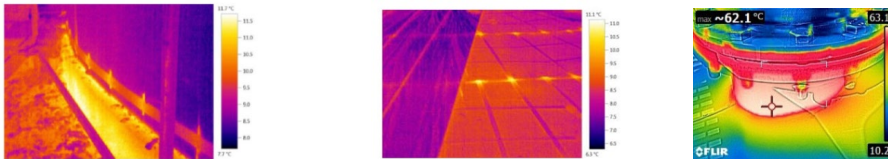
Fig. 4.1.1. Identified structural thermal bridges during accumulator construction (author's photos).

A thermal bridge is any element of increased thermal conductivity in a reservoir or it can occur as a result of inhomogeneous thermal insulation installation.
With thermal bridge the heat loss coefficient is calculated as H_T (W·K⁻¹), indicating energy loss (W)

$$H_T = \sum_i U_i\, S_i + \sum_i \psi_i\, l_i + \sum_k X_k, \qquad\qquad (4.1.1)$$

where ψ_i is calculated heat permeability (W·m^{-1}·K^{-1}) of linear thermal bridge j; l_i is designed lenght (m) of linear thermal bridge j ; and X_k is calculated heat permeability (W·K^{-1}) of dot point thermal bridge k [31].

The two-dimensional thermal bridges of the structure can be modulated and calculated, for example, using the THERM program according to the specified criteria. Using the THERM simulation calculation program allows classification of a high-precision method with an accuracy of ±5 % [34], but the possibility of error in determining thermal bridges is a major drawback.

By verifying the HS tank in this way in further operating modes, it is possible to accurately predict heat loss and costs.

Theoretical heat losses were calculated according to the methodology described in Chapter 3 under the experimental environmental conditions (the average approximate temperature during the experimental period was +17.09 ºC, the average wind speed was 3.14 m/s, temperature graph for HS in Fig. 4.1). Theoretical heat loss for this period was calculated to determine the correction factor n:

$$n = Q_{teor}/Q_{eksp} \times 100. \qquad\qquad (4.1.2)$$

According to this formula, Q_{teor}, $Q_{teor}+Q_{ter,til}$, Q_{eksp} were compared.
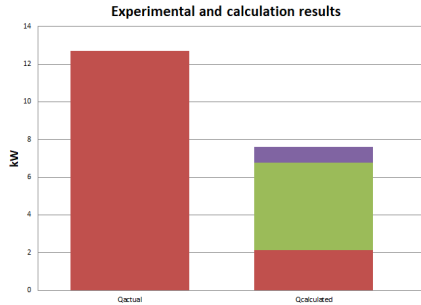
Fig. 4.1.2. Comparison of heat loss experiment and calculation results [62].

Figure 4.1.2 shows a comparison of HSs, where the 1st column is the experimentally obtained value of 12.71 kW. The second column is the theoretically calculated value of 7.59 kW without taking into account the thermal bridges. The result obtained during the theoretical calculations is 40.25 % lower if it is assumed that the thermal insulation is homogeneous and does not contain thermal bridges.

4.2. Conclusions of Chapter 4

The use of an experimental method to determine the actual heat loss under real conditions is more accurate than the search, modeling and calculation of thermal bridges. The author was the construction manager knowing the potential of the assembly and measuring the thermal chamber, therefore it was still possible to determine and calculate the large structural thermal bridges, but the inhomogeneous thermal assembly was impossible to measure due to the ventilated facade.

An experiment was performed during which heat accumulation was stopped and heat loss was observed for a period of 168 h. During this period, temperature drops were recorded and compared with the theoretical calculation. Observational data showed that under the experimental conditions, the battery lost heat with

12.79 kW. Performing the theoretical calculation under the experimental conditions and not taking into account the thermal bridges, a heat loss power of 7.59 kW was obtained.

A correction factor of 1.403 was introduced during the verification of the heat accumulator. Such verification of the heat loss of the heat accumulator is necessary in order to be able to implement this coefficient in the equations and integrate the in-depth analysis of the heat accumulator into the common cogeneration plant decision making algorithm.

5. FORECASTING OF HEAT LOAD

5.1. Forecasts of heat energy load

For the cogeneration plant in the free electricity market, one of the most important factors is to accurately forecast the heat load for the announced electricity production period. More importantly, in the case of cogeneration with heat storage, where heat forecasting affects the interaction between the two plants [22].

For heat sources and district heating networks (DHN), the operation is planned using forecasts, but the heating units of the buildings and buildings are regulated individually according to the actual heat demand. As a result, forecasts and actual district heating (DHS) loads can differ significantly [35].

Although in many studies in DHN load forecasting is performed on a daily basis, in order to plan the electricity generation schedule of a cogeneration plant for the wholesale electricity market, it is necessary to adapt the market-oriented operating and planning model to electricity trading platforms such as Nord Pool. To do this, the resolution of the forecast must be shifted to at least an hourly scale [35].

This chapter uses the heating load prediction algorithm, which is described and further developed to test its accuracy in DHS load prediction in a number of different systems during different heating seasons and with different model parameters. The obtained predicted deviations from actual consumption values are analyzed using the average percentage error of the error rate (MAPE) and the normalized average deviation error (NBIAS) [36].

5.2. Simple linear regression models of heat load

Table 5.2.1 shows the heating load of different city networks in the period of year December to March. Data for October to November and April were excluded because the heating load is not stable then. Table 5.2.1 provides an analysis of hourly heat load statistic data that allow to perform the linear regression of the heat load curves. Over a three-year period (2017–2019), data were obtained about two different DHSs with nominal capacity (RP, i.e., average consumption) ranging from 20 to 48 MW.

Table 5.2.1

Case Study Data for Different RP and Time Periods [36]

DHS RP/ number	Heating season	Average load Q_0, MWh/h	Minimal/ maximal load, MWh	Linear regression equation $(Q = aT + Q_0)$	R^2	Normalized slope, a/Q_0
RP20	2017–2018	18.56	14…38	$Q = -0.7972T + 18.563$	0.8770	−0.043
RP40	2017	42.41	22…80	$Q = -1.8123T + 42.407$	0.8579	−0.043
RP40	2018	40.94	12…75	$Q = -1.8357T + 40.937$	0.8977	−0.045
RP40	2019	41.95	22…62	$Q = -1.6395T + 41.946$	0.8039	−0.039
RP460	2015	457.48	210…1100	$Q = -22.877T + 457.48$	0.9400	−0.050

The regression analysis shown in Fig. 5.2.1 demonstrates how the heat load changes depending on the outside temperature. The goal of the analysis is to get as big as possible the sum of squares and draw a line according to the linear regression equation that best fits the collected DHS data.
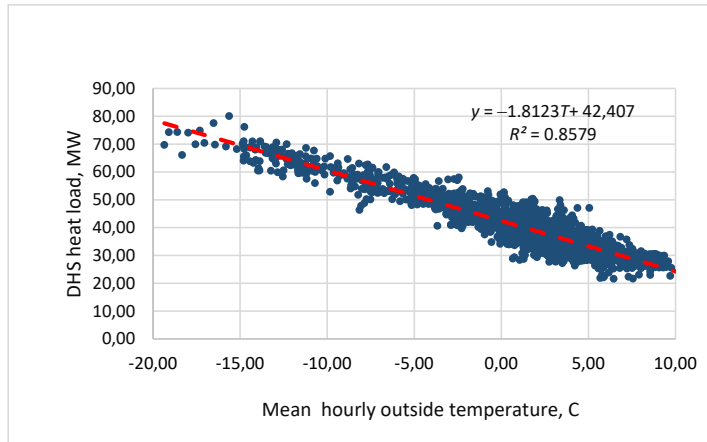
Fig. 5.2.1. DHS (RP = 40 MW) dependence on the external temperature in year 2017[36].

Each heating season had its own set of parameters (for example, air temperature profile), and therefore the linear regression equation for the same system may be different. In order to illustrate this, data on DHS with RP 40 MW were compared in three different heating seasons (2017, 2018, 2019), and the results were presented in Table 5.2.1 and Fig. 5.2.1.

The simple linear regression equations shown in the table represent the dependence of the heating demand on the outdoor temperature. In addition, Table 5.2.1 contains the coefficients of determination (R_2) for each case study, which is used as an indicator for the suitability of the determined linear equation. It shows the deviations of the measured DHS load from that calculated by the regression line. The value of R_2 is the sum of the squared deviations of the DHS load from the average value. The obtained regression models are generally considered to be strong if R^2 is close to 1. For example, in the case of RP20 in Fig. 5.2.1, the value of R^2 is 0.87, which is close enough to 1. In other cases, however, the coefficient is significantly lower. The linear regression of heating demand against the outdoor temperature usually shows a good correlation, however, when performing the analysis on a smaller scale (at the level of residential buildings), the correlation is significantly weaker. For example, the daily heat consumption R^2 versus air temperature was only 0.5459 [37]. However, on a larger scale, some consumer variances disappear to some extent, but the regression results for the overall system are much better. For example, for the second-order polynomial equations developed for the return temperature of heating networks [38], the detection factor was 0.9 from a function of air temperature.

However, there should be solved a situation that in most of the cases is presented in this chapter when the coefficient of determination of the linear regression equations is less than 0.9, and therefore it shows a larger difference between the obtained equation and the collected data. The R^2 value for the four studied DHS networks is from 0.9 to 0.8, or in other words, 10 % to 20 % of the calculated DHS load data.

5.3. Conclusions of Chapter 5

One of the most important factors for a cogeneration plant in the free electricity market is to accurately forecast the heat load for the next day. In the case of heat storage in a cogeneration unit, the heat load forecasts are even more important and the forecast resolution must be shifted to at least an hourly scale, as the parametric operating modes of the battery may result in losses due to an erroneous forecast [62].
The aim of the analysis was to obtain the least possible sum of squares and to draw a line according to the linear regression equation that best corresponds to the collected DHS data.

Possibilities to introduce a descriptive DHS parameter – normalized slope of the dimensionless heating curve, which is calculated as the ratio of the temperature coefficient of the linear regression equation to the average DHS heat load or *RP*, have been investigated. The analysis of statistical data provided by heat loads shows that for simple linear regression the coefficient of heat load of different Latvian DHS depending on the outdoor air temperature is in the range from 0.8 to 0.94.

6. OPTIMIZATION OF COGENERATION PLANT DECISION-MAKING ALGORITHM USING DEEP ANALYSIS OF HEAT ACCUMULATOR AND INCLUDING LOSS MODEL

The liberalization of the energy market and the EU's set targets for improving energy efficiency in each Member State [4] are contributing to the rapid development of heat accumulation facilities. Accurate production planning is very important in cogeneration plants operating in the free electricity market [40], [53], besides the use of heat accumulators increases significantly in terms of both complexity and additional calculation functions. In addition, the production process is affected by variable heat, CO_2 and fuel costs [41].

Reorientation to market conditions requires new challenges for CHP operational planning [40], such as next day weather and heat forecasts [45], or, for example, the planning of equipment operating costs depending on start-up (cold, warm, hot) conditions [46]. The accuracy of the forecasts influences the heat and power generation regimes of CHP [47] and, consequently, the strategies for determining free market volumes [48]. An artificial neural network model for heat demand in the district heating network is used for forecasting. In turn, different forecasting models are used for the price of electricity – extreme training machines, multilayer perceptrons, automatic ARIMA and triple exponential smoothing methods [45]. The analysis of historical data contributes to the development and accuracy of these methods and tools. Determining market volumes in the next day market takes place in a short time with a large amount of data input, therefore, forecasting tools in combination with multi-stage programming modeling concept methods already provide a reliable result and decision [49], [50]. By acquiring more effective CHP operation, there decarbonisation is promoted [51] and the use of HS can improve the efficiency of the whole plant [52]. The use of HS as a system element affects the performance of the whole system [45], increases the uncertainty for the efficient use of the equipment if not all criteria, such as losses, are considered [54]. The calculation of the impact of electrical and heat loss costs of the HS operating mode included in the cost model has been performed.

A decision-making algorithm for cogeneration plants for the free market conditions of electricity has been developed, which is based on the cost of electricity and a detailed analysis of HS with the included operating cost model. The algorithm serves as a short-term computer systems planning tool, the aim of which is to maximally increse the total gross revenue limit for the planning of cogeneration operations and to exclude such operating modes that may cause losses.

The efficient operation of the installed heat accumulation system is influenced by factors such as the actual heat capacity, charging, discharging rates and the ability to determine whether the unit meets the specified operating mode. The operating mode depends on the flow and return temperatures T_1, T_2, and the height of HS thermal wedge with temperature T_3. In turn, the operator must also take into account for operation planning such factors as HS heat loss, which depends on the thermal insulation resistance from the $T_{externalair}$, wind exposure, electricity consumption in addition to the operation of pumps No. 1, 2, 3, 4 to ensure the process and equipment maintenance costs. In addition, when CHP is working in the next day's market, the planning of HS's operations requires an hourly forecast for the next 24 hours, where the prices of electricity, heat, CO_2 emissions (if fossil fuels) and fuel are variable in free market conditions.

The scheme of a biomass cogeneration plant with a heat accumulator is shown in Fig. 6.1, where the author performed an in-depth analysis of this element.

Fig. 6.1. The scheme of a biomass cogeneration plant with a heat accumulator [25].

6.1. Cost model of heat accumulator operation mode

The use of a heat accumulator must not impair the overall efficiency of the CHP [39], where $Re^{KS} < Re^{KS} + Re^{HS} - C_{total}$ (expenses for provision of process). The main costs in this model are electricity, heat loss and maintenance and repair, which are expressed by the formula:

$$C_{total} = C_{heat} + C_{el} + C_{maintenance\ costs} \qquad (6.1)$$

The methodology developed by the author for calculating heat loss is shown in Chapter 4, where heat loss of 438 kwh was obtained and heat loss is determined:

$$C_{sil} = Q_{sil} \times C_{pp\ h} \qquad (6.2)$$

Biomass cogeneration plants with heat accumulator operate three pumps to ensure the process.
Pump No. 2 with an electrical capacity of 75 kw is working at heat energy charging.
Pump No. 1 with el. power 200 kw and pump No. 3 with electrical power 30 kw are working at discharging.

$$C_{el} = P \times h \times C_{pp\ el} \ , \qquad (6.3)$$

where P is power, kwh, and h is number of working hours.

Analyzing HS operation in maximum mode for 12 hours charging and 12 discharge modes is as follows.
Maximal charging process:
$Q_{Pump\ No.\ 2} = 75 \times 12 = 825$ kWh
Maximal discharging process:
$Q_{Pump\ No,\ 1}\ Q_{Pump\ No.\ 3} = 200 \times 12 + 30 \times 12 = 2200 + 330 = 2530$ kWh

In order to evaluate the efficiency of the HS accumulator, the costs of system maintenance, repair and system availability should not be disregarded. The HS system includes a large number of devices, such as pumps, valves, meters, sensors and other equipment for operation. These, including devices, require regular maintenance, otherwise failures may occur that will affect the production process.

Asset management systems allow you to manage, plan and track work and the resources needed to complete it. Skillful maintenance of physical assets ensures that the volume of emergency work does not exceed 10 % of the total work. World experience shows that companies are able to achieve technical availability of up to 98.6 % [27].
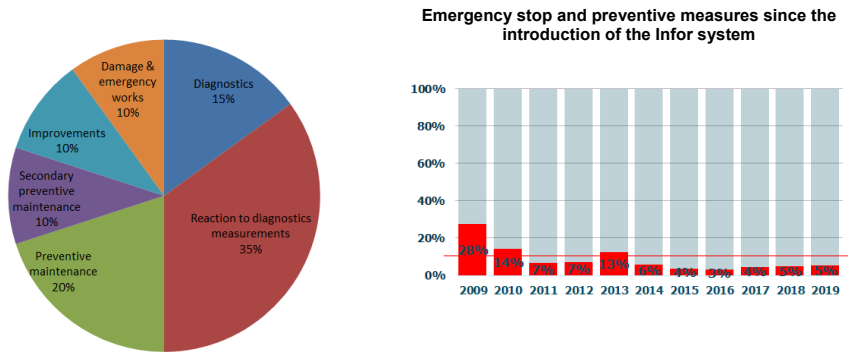
Fig. 6.1.1. Time distribution of the asset management system implemented by "Industry Service Partner" Ltd for a change in the dynamics of production processes [28].

Figure 6.1.1 shows the asset management system Infor implemented by "Industry Service Partner" Ltd and the dynamics of failures during 10 years. Initially, in 2009, the company's equipment failures accounted for as many as 28 % of cases. The graph shows that the failures in such a company have been reduced 2 times in the first year and have stabilized over 5 years and account for an average of 5 % of the total equipment maintenance time. The rest of time or 95 % is taken for preventive measures.

The average service costs per day are calculated:

$$C_{\text{maintenance costs}} = C_{\text{yearly maintenance costs}}/h, \tag{6.4.}$$

where h is yearly hours of operation.

6.2. Decision-making algorithm

Based on the five-level *Functional Scheme* (Fig. 1.2.2), a multi-level Euclidean block diagram decision-making algorithm of CHP operating with HS was developed using the factors shown in Fig. 6.2.1. Figures 4.1 and 4.2 complement each other, where in Fig. 4.1, the main input data and 4 output functions are displayed. In turn, Fig. 4.2 shows the calculation sequence and output functions of influencing factors Yes/No. In Fig. 4.2, the main emphasis of the algorithm is on the inclusion of the data of in-depth analysis of the HS, as a result of which the operating costs of the CHP are specified in order to exclude such operating modes that cause losses in the operation of the HS.

To get a positive result, where the use of HS is efficient and profitable, you must pass a 12-position filter. The algorithm can also lead to the following results: CHP operation without HS; CHP operation only for self-consumption electricity production; and production of electricity is not economically viable. At the initial starting position, the availability of CHP equipment must be assessed. In addition, it is necessary to identify the risks and whether the technical condition does not pose a hazard that can affect the production process [27].

1. The starting position begins with a calculation of the cost of electricity production ($C_{\text{pp el}}$). Production costs are affected by many factors, such as CO_2 stock prices, heat tariff, cogeneration efficiency, fuel and personnel costs, and other factors [61].

2. The availability of CHP equipment must be assessed in this block. In addition, it is necessary to identify the risks and whether the technical condition does not pose a hazard that will affect the production process [27].

3. Initially, the market price of electricity must be forecasted for the whole period of the day and compared with the production costs. This step determines whether the market price of electricity per hour is higher than the cost of electricity production:

$$C_{\text{mp el}}\, \boldsymbol{nh} > C_{\text{pp.}} \qquad\qquad (6.1)$$

If the cost of electricity generation $C_{\text{pp el}}$ is higher than the daily hourly forecasted, then it is not effective to use HS for revenue generation. A situation may arise where the operation of the CHP is economically inefficient or it is possible only to cover the needs of the CHP for own consumption. In addition, it must be taken into account whether the technological minimum capacity of the generator corresponds to self-consumption and if the purchased electricity from the network is cheaper than the cost price of the produced one.

4. In a situation where the price in the next day's electricity market is equal to or almost equal to the average market price for the entire 24-hour period, the operation of the HS equipment is inefficient and its charging and discharging is unfavorable due to heat and electricity losses:

$$\overline{(Cmp)} \neq C_{\text{mp}}\mathbf{1}\text{h} \approx C_{\text{mp}}\boldsymbol{nh} \approx C_{\text{mp}}\mathbf{24}\text{h}. \qquad\qquad (6.2)$$

In this case, the result is obtained showing that the operation of the CHP should be organized without HS.

5. The best average stock market price is calculated over a period of time above the electricity production price $\overline{(Cmp)}_{\text{best max period}}$:

$$\overline{(Cmp)}_{\text{bestmax.period}} = (C_{\text{mp}}\mathbf{1}\text{h} + C_{\text{mp}}\mathbf{2}\text{h} + C_{\text{mp}}\boldsymbol{nh})/\boldsymbol{nh}. \qquad\qquad (6.3)$$

This function determines the best period during which the operation of CHP under market conditions can bring the highest income in the operation of both CHP and CHP with HS.

6. In addition to the electricity market price, it is important to forecast also the next day's heating demand before deciding whether the heat storage operation could be profitable. Accurate heat load forecasting has a significant impact on the entire production planning process. It is very important to forecast the heat load for every hour for the next 24 hours and to determine the flow and return temperatures of the network. This is due to the period announced by the stock market for the next day at 12:00 on the current day [8]. This means that as a result of an inaccurate forecast, the heat accumulator may be prematurely charged, then there will be nowhere to utilize the heat produced and the cogeneration production capacity will have to be reduced. A situation may also arise that if all the energy from the HS is not discharged during low hours of the electricity market, then in the case of the next applied cycle, it will not be possible to charge the HS to the expected amount. This means that produced electricity will not be produced in the amount of the applied capacity, where with a good electricity price, there will be not only the lost profit, but also unproduced amount will have to be compensated [8].

7. In case the forecasted heat load corresponds to the maximum capacity of the CHP or is higher, then the cogeneration block can be loaded in the desired mode in the maximum market price range and it is not expedient to use HS for profit generation.

8. Depending on the heat and electricity production ratio and the flexibility of the production blocks, a calculation has to be made to decide on the operating hours of the CHP per hour. In addition, the conditions for starting (cold, warm, and hot) and increasing or decreasing the capacity of the cogeneration unit should should as well be taken into account in ideal situation [39]. This block also determines the need for self-consuming Psc electrical energy to ensure the process.

START

1. Calculates the current production cost of electricity CP el

2. Is CHP available — YES / NO

3. Market hourly price Cmpnh>CP el — YES / NO

4.

5. Calculate the best period of the average best market price $\overline{(Cmp)}_{bestmax.period}$

$\overline{(Cmp)}_{best\ max.period} \neq$ Cmpnh — YES / NO

6. Heat demand forecasted for DAY-AHEAD period $\overline{Q}_{DH}$

Heat demand for DAY-AHEAD period $\overline{Q}_{DH}$

Calculate self-consumption of eletricity Pscnh

7. $\overline{Q_{DH}} \neq<$ CHP max heat demand Phmax — YES / NO

CHP min el.power $P_{min\ gen}<P_{sc}$nh — YES / NO

8. Calculate/Recalculate: $\overline{Pel}_{max.}$ $\overline{Pheat}$, every h self-consumption of eletricity Pscnh

Calculate Re el

9. Calculate Re HS

CP el< C network el — YES / NO

Re el <Re HS — YES / NO

10. Is HS available — YES / NO

11. HS heat capacity forecast $(Q_{foresc.HS}-Q_{hs\_actua})>$ charge/discharge $(P_{char(forecasted)}$xh-$P_{disch(forecasted)}$xh) — NO / YES

Calculate HS operating costs

CHP operation for self-consumption eletricity

12. Re el-Costs > Re HS - Costs (HS operating) — YES / NO

HS is not efficient, cogeneration modes **without HS**

CHP's operation with HS is justified and cost-effective

Calculate $\overline{Pel}_{max.}$ $\overline{Pheat}$, every h self-consumption for eletricity Pscnh

Recalculation Re el

Produce el. not economically benefical

END

Fig. 6.2.1. Block scheme of decision-making algorithm.

9. In this block, two revenue figures Pr^{el} are defined, where the maximum revenue for CHP operation without HS and Pr^{hs}, where CHP operation with HS.

In this calculation block, two revenue figures Pr^{el}, where or the maximum revenue in CHP operation without HS and Pr^{hs}, where or CHP in operation with HS, are determined.

10. The availability of HS equipment must be assessed in this block. In addition, it is necessary to identify the risks whether the technical condition does not pose a hazard that can affect the production process [27].

11. In this block, it is calculated if the remaining heat in the HS and the forecasted CHP mode with the produced additional heat ensures the charging of the HS and later the maximum discharge. These parameters can vary depending on the forecasted heating network temperature schedule. It may be that the heat capacity of the HS does not allow to perform the storage of all heat generated in the electricity production mode, or, if all the heat in the accumulator is not used in night mode, additional calculation is required for CHP operation to adapt the mode to the current and forecasted HS situation.

12. In this block, the evaluation of the cost model of heat accumulator operation modes performed in Chapter 3 is applied. Total losses are deducted from revenue. Only income from CHP and CHP with loss are compared. Output function – the operation of the HS is effective, or the losses account for a larger share than the revenue, then the operation of the CHP without the HS is recommended.

6.3. Conclusions of Chapter 6

The decision-making algorithm of the cogeneration plant in operation with heat accumulators has been optimized by performing a deep analysis of the accumulator and introducing its parametric functions. The algorithm results in 4 output states or results: CHP operation with HS; CHP operation without HS; CHP operation for providing self-consumption; and it is not profitable to produce electrical energy. It will provide maximum revenue and will quickly exclude such operating modes that could bring losses in the free electricity market. The heat accumulation calculation module includes not only heat capacity, charge-discharge capacities, and heat losses, but also the following parametric functions:

- Including the HS operating mode cost model in the algorithm showed that the highest costs are those of electricity consumption, where 3.355 MWh was consumed in the operating mode to ensure operation. The heat loss for the calculated operating mode was 0.43 MWh.
- The algorithm includes HS availability and maintenance costs. This part is insignificant in relation to total operating costs, but has a significant impact on production planning if there are risks of refusal. The introduction of an asset management system in the company helps to reduce the time spent on repairs of emergency equipment by up to 5 times. Increasing the number of preventive measures and diagnostics can significantly increase the availability of equipment and common systems.

7. CONCLUSIONS

1. The analysis of the literature shows that the loss of MP support for cogeneration modes is affected not only by the changing heat load, but also by the volatile electricity market. As a result of many variables, it is difficult to make a production decision if it has to be made the next day, which must be done in the free market of electricity from 10:00–12:00 on this day, where demand and supply are created on the exchange. In addition, the use of heat storage and heat pump technology further increases uncertainty, as the technical and economic parameters of the equipment also need to be planned under changing market and environmental conditions. For example, heat accumulator technology can increase the efficiency of a heat source, but without planning and technological calculations can reduce efficiency or cause losses.
Five large basic blocks for the algorithm were defined – electricity cost costs, electricity market prices, heat load, cogeneration operation mode and heat accumulator calculation modules, which influence the cogeneration plant production decisions most. Each of the modules forms calculation processes, where the input data and equations form output functions with five states that define an economically sound production decision.

2. Increased efficiency, reduced emissions and heat load balancing can be achieved by upgrading plants with heat storage and heat pump technology during the operational phase.
   2.1. Deep flue gas cooling with an absorption heat pump has a wide range of applications, e.g., in cogeneration and water heating boilers to improve efficiency. There are many components of efficient energy recovery from flue gases (flue gas condensers, absorption coolers, heat exchangers, etc.). There are still not enough studies to determine the rated capacity of a heat pump for different operating conditions. Experimental and theoretical calculation data show that the thermal efficiency of the boiler can be improved by up to 16 % if the flue gas temperature is reduced to 25 °C.

   2.2. Analysis of real data shows that electricity prices at night are often lower, but at this point the heat load increases, while during the day hours at lower heat load, electricity prices reach their peaks. Temporary heat accumulation allows to balance the heat load and accumulate additional heat during the day. The study shows that the use of heat storage equipment in a cogeneration plant with cogeneration units with a total electrical capacity of 2.64 MW$_{el}$ enables the production and sale of up to 4272 MWh of additional electricity per year at the existing heat load. In the case of fossil fuels, 959 t CO_2 emissions are saved.

3. Determining the theoretical heat loss for heat storage in operating modes requires extensive multi-step calculations, as many factors such as thermal insulation resistance, variable internal temperature changes, free and forced convection, outdoor temperature, wind, and other factors must be taken into account. Important is not only the calculation of heat loss, but also the height of the thermal wedge. In addition, the height of the thermocline affects heat loss in different operating modes but can reduce or increase the heat capacity of the battery. The height of the thermal wedge is influenced by such factors as the ratio of the height and diameter of the heat accumulator and thermal insulation efficiency. A multi-stage heat loss and thermocline calculation methodology was developed to be able to integrate these equations as part of a module for in-depth analysis of a heat accumulator in a common cogeneration plant decision-making algorithm.

   3.1. When collecting data for three Latvia's largest heat accumulators and their thermal insulation solutions, it was found that different solutions were used, including thickness. For example, the heat transfer coefficient U of the roof of object X with a thickness of 0.5 m is the best 0.089 W/(m^2·K), while for the walls it was the worst – 0.122 W/(m^2·K). The different thermal insulation solutions in the calculations showed that the values of coefficient U are very close, and

in the modulation of the 24-hour operating mode at the same parameters, a difference of 2.8 % in heat loss was obtained between the objects. The lowest heat losses were for the thermal insulation solution of object Y with 314.29 kWh.

4. The use of an experimental method to determine the actual heat loss under real conditions is more accurate than the search, modeling and calculation of thermal bridges.
    An experiment was performed during which heat accumulation was stopped and heat loss was observed for a period of 168 h. During this period, temperature drops were recorded and compared with the theoretical calculation. Observational data showed that under the experimental conditions, the accumulator lost heat with 12.79 kW. Performing the theoretical calculation under the experimental conditions and not taking into account the thermal bridges, a heat loss power of 7.59 kW was obtained.
    A correction factor of 1.403 was introduced during the verification of the heat accumulator. Such verification of the heat loss of heat accumulator is necessary in order to be able to implement this coefficient in the equations and integrate the deep analysis of the heat accumulator into the common cogeneration plant decision-making algorithm.

5. One of the most important factors for a cogeneration plant in the free electricity market is to accurately forecast the heat load for the next day. In the case of heat storage in a cogeneration unit, the heat load forecasts are even more important and the forecast resolution must be shifted to at least an hourly scale, as the parametric operating modes of the battery may result in losses due to an erroneous forecast [62].
    The aim of the analysis was to obtain the least possible sum of squares and to draw a line according to the linear regression equation that best corresponds to the collected DHS data.
    Possibilities to introduce a descriptive DHS parameter – normalized slope of the dimensionless heating curve, which is calculated as the ratio of the temperature coefficient of the linear regression equation to the average DHS heat load or RP, have been investigated. The analysis of statistical data provided by heat loads shows that for simple linear regression the coefficient of heat load of different Latvian DHSs depending on the outdoor air temperature is in the range from 0.8 to 0.94.

6. The decision-making algorithm of the cogeneration plant in operation with heat accumulators has been optimized by performing a deep analysis of the accumulator and introducing its parametric functions. The algorithm results in 4 output states or results: CHP operation with HS; CHP operation without HS; CHP operation for providing self-consumption; and not profitable to produce electrical energy. It will provide maximum revenue, will quickly exclude such operating modes that could bring losses in the free electricity market. The heat accumulation calculation module includes not only heat capacity, charge-discharge capacities, and heat losses, but also the following parametric functions:

    - Icluding the HS operating mode cost model in the algorithm showed that the highest costs are those of electricity consumption, where 3.355 MWh was consumed in the operating mode to ensure operation. The heat loss for the calculated operating mode was 0.43 MWh.
    - The algorithm includes HS availability and maintenance costs. This part is insignificant in relation to total operating costs but has a significant impact on production planning if there are risks of failure. The introduction of an asset management system in the company helps to reduce the time spent on repairs of emergency equipment by up to 5 times. Increasing the number of preventive measures and diagnostics can significantly increase the availability of equipment and common systems.

USED LITERATURE

1. *Enerģētikas likums* (1998) [tiešsaiste]. LR likums Rīga: pieņemts Rīgā 1998. gada 3. septembrī, Latvijas Vēstnesis, interneta vietne Likumi.lv [skatīts 2018. g. 1. martā]. Pieejams: https://likumi.lv/doc.php?id=49833

2. *Likums par Latvijas Nacionālo enerģētikas un klimata plānu 2021.–2030. gadam.* (2020) [tiešsaiste]. LR likums Rīga: pieņemts Rīgā 2020. gada 4. februārī, Latvijas Vēstnesis, interneta vietne Likumi.lv [skatīts 2018. g. 1. martā]. Pieejams: https://likumi.lv/ta/id/312423-par-latvijas-nacionalo-energetikas-un-klimata-planu-20212030-gadam

3. *Parīzes nolīgums – ANO Vispārējā konvencija par klimata pārmaiņām* [tiešsaiste]. Brisele, ratificēts ES 2016. gada 5. oktobrī, Oficiāla Eiropas Savienības tīmekļa vietne [skatīts 2018. g. 1. martā]. Pieejams: https://eur-lex.europa.eu/content/paris-agreement/paris-agreement.html?locale=lv

4. *Klimata un enerģētikas satvars laikposmam līdz 2030. gadam* [tiešsaiste]. Brisele, pieņemts ES 2014. gada 23. oktobrī, oficiāla Eiropas Savienības tīmekļa vietne [skatīts 2020. g. 1. novembrī]. Pieejams: https://www.consilium.europa.eu/lv/policies/climate-change/2030-climate-and-energy-framework/

5. *Likums par Ppr Apvienoto Nāciju Organizācijas Vispārējo konvenciju par klimata pārmaiņām* [tiešsaiste]. LR likums Rīga: pieņemts Rīgā 1995. gada 3. septembrī, Latvijas Vēstnesis, interneta vietne Likumi.lv [skatīts 2018. g. 1. martā]. Pieejams: https://likumi.lv/ta/id/34198-par-apvienoto-naciju-organizacijas-visparejo-konvenciju-par-klimata-parmainam

6. *Eiropas zaļais kurss un pakete "Gatavi mērķrādītājam 55 %"* [tiešsaiste]. Brisele, pieņemts ES Vides padomē 2022. gada 17. martā, Oficiāla Eiropas Savienības tīmekļa vietne [skatīts 2022. g. 18. Martā]. Pieejams: https://www.consilium.europa.eu/lv/policies/green-deal/timeline-european-green-deal-and-fit-for-55/

7. *Metroloģisko novērojumu dati* [tiešsaiste]. Rīga, 2018. Latvijas Vides, ģeoloģijas un meteoroloģijas centra tīmekļa vietne videscentrs.lvgmc.lv [skatīts 2018. g. 1. martā]. Pieejams: https://www.meteo.lv/meteorologija-datu-meklesana/?nid=461

8. *Elektroenerģijas cenas biržā* [Tiešsaiste]. Ziemeļu un Baltijas reģions Nord pool birža, 2021 [skatīts 2021. g. 1. decembrī]. Pieejams: https://www.nordpoolgroup.com/historical-market-data/

9. Henrik, L., Østergaard, P. A., Connolly, D., Ridjan, I.,. Mathiesen, B. V., Hvelplund, F., Thellufsen, J. Z., Sorknæs, P. Energy Storage and Smart Energy Systems. I*nternational Journal of Sustainable Energy Planning and Management.* 2016.11.211: 3–14. doi:10.5278/ijsepm.

10. H. Lund, S. Werner, R. Wiltshire, S. Svendsen, J. Thorsen, F. Hvelplund and M. B. V., 4th Generation District Heating (4GDH) Integrating Smart Thermal Grids Into Future Sustainable Energy Systems. *Energy*. 2014; 68: 1–11.

11. Buffaa, S., Cozzinia, M., D'Antonia, M., Baratierib, M., Fedrizzia, R., 5th generation district heating and cooling systems: A review of existing cases in Europe. *Elsevier*. 2019, vol. 104(C), pp. 504–522.

12. Bertelsen, N., Petersen, U. R. Thermal Energy Storagein Greater Copenhagen. Master's Thesis MSc in Engineering Sustainable Cities Department of Planning. Denmark, University Copenhagen, 2017.

13. Pinel, P., Cynthia, A. Cruickshank, Ian Beausoleil-Morrison, Adam Wills. A review of available methods for seasonal storage of solar thermal energy in residential applications. Renewable and Sustainable Energy Reviews. 2011; vol 15 pp. 3341-3359

14. Hou, J., Che, D., Liu, Y., Jiang, Q. A new system of Absorption Heat Pump Vs. Boiler for recovering Heat and water Vapor in Flue gas. *Energy Procedia*. 2018, vol. 152, pp. 1266–1271.

15. Che, D., Liu, Y., Gao, C. Evaluation of retrofitting a conventional natural gas-fired boiler into a condensing boiler. *Energy Convers Manage.* 2004, vol. 45, pp. 3251–3263.

16. Westerlund, L., Hermanson, R., Fagerström, J. Flue gas purification and heat recovery: A biomass fired boiler supplied with an open absorption system*. Applied Energy*. 2012, vol. 96, pp. 444–450.

17. Yang, B., Jiang, Y., Fu, L., Zhang, S. Conjugate heat and mass transfer study of a new open-cycle absorption heat pump applied to total heat recovery of flue gas. Applied Thermal Engineering. 2018, vol. 138, pp. 888–899.

18. Yang, B., Yuan, W., Fu, L., Zhang, S., Wei, M., Guo, D. Techno-economic study of full-open absorption heat pump applied to flue gas total heat recovery. *Energy.* 2020, vol. 190, 116429

19. Sauhats, A., Dolgicers, A., Kozadajevs, J., Zālītis, I., Boreiko, D. The Impact of the District Heating System Thermal Inertia on the CHPP Operation Mode. *In: 2019 IEEE 60th International Scientific Conference on Power and Electrical Engineering of Riga Technical University (RTUCON):* Conference Materials, Latvia, Riga, 7–9 October 2019. Piscataway: IEEE, 2019, pp. 225–229. ISBN 978-1-7281-3943-2

20. Sauhats, A., Kozadajevs, J., Dolgicers, A., Zālītis, I., Boreiko, D. Thermal Energy Storage for CHP in Power Market Conditions. *16th European Energy Market Conference.* 2019. September, (EEM 2019), Slovenia, Ljubljana, pp. 18–20.

21. Rusovs, D., Zentins, V. Steam driven absorption heat pump and flue gas condenser applied for heat recovery in district heating network. *19th International Scientific Conference Engineering for Rural Development* 2020, Jelgava, pp. 1627–1632. ISSN 1691-5976

22. Soročins, A., Rusovs, D., Nagla, J., Žentiņš, V. The Influence of the Thermal Storage on the Electricity Production in a Co-Generation in Peak and Off-Peak Time Range. *2020 IEEE 61st International Scientific Conference on Power and Electrical Engineering of Riga Technical University (RTUCON 2020)*: 5–6 November 2020, Riga, Piscataway: IEEE, 2020, pp. 136–139. ISBN 978-1-7281-9511-7

23. Kavvadias, K., Jimenez Navarro, J. P., Zucker, A., Quoilin, S. Case study on the impact of cogeneration and thermal storage on the flexibility of the power system. *Joint Research Centre.* 2017. Tech. rep. Luxembourg, doi: 10.2760/814708.

24. Latvijas Vides, ģeoloģijas un meteoroloģijas centrs, CO2 emisiju no kurināmā stācionārās sadedzināšanas āprēķinu metodika, Rīga, 2020. gada janvāris.

25. Cimdina, G., Blumberga, D., Veidenbergs, I. Analysis of wood fuel CHP operational experience, International Scientific Conference "Environmental and Climate Technologies – CONECT 2014, Energy Procedia 72 (2015) 263–269, Riga.

26. *Akumulatora izbūve* [tiešsaiste]. Jelgava, 28.02.2019. [skatīts 2020 .g. 1. novembrī] Pieejams: https://www.jelgava.lv/lv/jaunumi/zinu-arhivs/siltumapgades-uznemums-fortum-jelgava-buve-siltumenergijas-akumulatoru/

27. Raikar, V. A., Naik, G., Naik, P., A Simulation Model for Overall Equipment Effectiveness of a Generic Production Line. OSR Journal of Mechanical and Civil Engineering (IOSR-JMCE). Sep. – Oct., 2015, e-ISSN: 2278-1684,p-ISSN: 2320-334X, Volume 12, Issue 5, Ver. III, pp. 52–63.

28. Neilands, R., Šaršuns, N., Automatic monitoring and control system, Wastewater treatment process supervision in Riga city."Industry Service Partner" Ltd presentation. Riga, 1 October 2020.

29. Nagla, J., Saveljevs, A., Ciemins, R., Siltumtehnikas pamati, Rīga "Zvaigzne", 1981.

30. Žentiņš, V., Rusovs, D., Soročins, A., Cars, A., Analysis of different thermal insulation solutions of a heat storage. *Riga Technical University 62nd International Scientific Conference*. 15 October 2021, 5 p, ISBN 978-9934-22-756-1

31. Ekonomikas ministrija, Metodiskie norādījumi Latvijas būvnormatīva LBN 002-01 „Ēku norobežojošo konstrukciju siltumtehnika", Rīga, 2005.

32. Fundamentals of Heat and Mass Transfer, 7th Edition. Theodore L. Bergman, Adrienne S. Lavine, Frank P. Incropera. John Wiley & Sons, Incorporated, 2011. ISBN 0470501979, 9780470501979

33. U.S. Department of Energy, Thermodynamics, Heat Transfer and Fluid Flow. DOE Fundamentals Handbook, Volume 2 of 3. May 2016.

34. European Committee for Standardization, Thermal bridges in building construction – Linear thermal transmittance – Simplified methods and default values, LVS EN ISO 14683:2008, 2007.

35. Baltputnis, K., Petričenko, R., Soboļevskis, D. Heating Demand Forecasting with Multiple Regression: Model Setup and Case Study. In: 2018 IEEE 6th Workshop on Advances in Information, *Electronic and Electrical* Engineering (AIEEE 2018), Lithuania, Vilnius, 8–10 November 2018. Piscataway, NJ: IEEE, 2018, pp. 91–95. ISBN 978-1-7281-2000-3Lithuania

36. Rusovs, D., Jakovļeva, L., Žentiņš, V., Baltputnis, K. Heat Load Numerical Prediction for District Heating System Operational Control. *Latvian Journal of Physics and Technical Sciences.* 2021, Vol. 58, No. 3, pp. 121–136. ISSN 0868-8257. Available: doi:10.2478/lpts-2021-0021.

37. Blumberga, D., Blumberga, A., Vitolins, V. *Energy audits in dwelling buildings in Latvia. Data analysis.* [Accessed 20 december 2020]. Riga, 2005. Available: https://docplayer.net/18489666-Energy-audits-in-dwelling-buildings-in-latvia-data-analysis.html

38. Talcis, N., Dzelzītis, E., Līckrastiņa, A.. Return Temperature in DH as Key Parameter for Energy. *International Journal of Modern Engineering Research.* (2018) 8 (7), pp. 88–92.

39. Ivanova, P. Termoelektrocentrāļu elastīguma un efektivitātes palielināšana mainīgos darbības apstākļos. *Promocijas darba kopsavilkums.* Rīgas Tehniskās universitātes izdevniecība, 2018.

40. Dvorák, M., Havel, P., Combined heat and power production planning under liberalized market conditions Applied Thermal Engineering, Volume 43, October 2012, pp. 163–173.

41. Lam, L. H., Valentin, I., Bovo, C., European day-ahead electricity market coupling: Discussion, modeling, and case study. *Electric Power Systems Research.* February 2018.

42. LR Centrālā statistikas pārvalde, 19.05.2020 [skatīts 2020. 20. Decembrī]. Pieejams: https://www.csb.gov.lv/lv/statistika/statistikas-temas/vide-energetika/energetika/meklet-tema/2685-kogeneracijas-staciju-darbiba-2019-gada

43. LR Ekonomikas Ministrija, preses relīze 16.07.2020. [skatīts 2020. 20. Decembrī] Pieejams: https://www.em.gov.lv/lv/sogad-atbalstu-zaudejusas-10-oik-elektrostacijas-valsts-ietaupijusi-1463-milj-eur

44. LR Ekonomikas ministrija preses relīze 22.09.2020. [skatīts 2020. 21. Novembrī] Pieejams: https://www.mk.gov.lv/lv/aktualitates/valdiba-lemj-par-talakajiem-soliem-oik-samazinasanai

45. Zymełka, P., Szega, M., Short-term scheduling of gas-fired CHP plant with thermal storage using optimization algorithm and forecasting models. *Energy Conversion and Management.* March 2021, Volume 231, 1, 113860.

46. Mitra, S., Sun, L. E., Grossmann I., Optimal scheduling of industrial combined heat and power plants under time-sensitive electricity prices. *Energy.* June 2013, Volume 54, pp. 194–211.

47. Atănăsoae, P., The Operating Strategies of Small-Scale Combined Heat and Power Plants in Liberalized Power Markets. *Energies.* 2018. 11, 3110; doi:10.3390/en11113110.

48. Cui, H., Song, K., Dou, W., Nan, Z., Wang, Z., Zhang, N., Bidding Strategy of a Flexible CHP Plant for Participating in the Day-Ahead Energy and Downregulation Service Market. *Journal IEEE ACESS.* 1 October 2021, pp. 49647–149656, ISSN: 2169-3536DOI: 10.1109/ACCESS.2021.3116981

49. Kumbartzky, N., Schacht, M., Schulz, K., Werners, B., Optimal operation of a CHP plant participating in the German electricity balancing and day-ahead spot market. *European Journal of Operational Research.* Volume 261, Issue 1, 16 August 2017, pp. 390–404.

50. Schledorn, A., Guericke, D., Andersen, A. N., Madsen, H., Optimising block bids of district heating operators to the day-ahead electricity market using stochastic programming, *Smart Energy.* February 2021, Volume 1, 100004.

51. Koch, K., Alt, B., Gaderer, M., Dynamic Modeling of a Decarbonized District Heating System with CHP Plants in Electricity-Based Mode of Operation. *Energies.* 2020, 13, 4134; doi:10.3390/en13164134.

52. Fang, T., Lahdelma, R., Optimization of combined heat and power production with heat storage based on sliding time window method, *Applied Energy.* 15 January 2016, Volume 162, pp. 723–732.

53. Al-Mansoura, F., Kožuh, M., Risk analysis for CHP decision making within the conditions of an open electricity market. Energy. (2007), 32, 1905–1916.

54. Zheng, P., Liu, P., Zhang, Y., Economic Assessment and Control Strategy of Combined Heat and Power Employed in Centralized Domestic Hot Water Systems, Appl. Sci. 2021, 11(10), 4326.

55. Fan, J., Furbo, S., Thermal stratification in a hot water tank established by heat loss from the tank. *Renewable Energy Shaping Our Future Proceedings of the ISES Solar world congress Johannesburg, South Africa.* 2009. pp. 341–350. ISBN 978-1-920017-42-2

56. Haller, M. Y., Yazdanshenas, E., Andersen, E., Wolfgang Streicher, C. B., Furbo, S., A method to determine stratification efficiency of thermal energy storage processes independently from storage heat losses. Solar Energy. 2010. ISSN 0038-092X, E-ISSN 1471-1257, Vol. 84, no. 6, pp. 997–1007.

57. Karim, A., Burnett, A., Fawzia, S. Investigation of Stratified Thermal Storage Tank Performance for Heating and Cooling Applications. *Energies.* 2018, Vol. 11, p. 1049.

58. Ying, L., Fengzhong, S., Qiannan, Z., Xuehong, C., Wei, Y. Numerical Simulation Study on Structure Optimization and Performance Improvement of Hot Water Storage Tank in CHP System. *Energies.* 2020, Vol. 13(18), p. 4734.

59. Henrik, L., Østergaard, P. A., Connolly, D.,Ridjan, I., Mathiesen, B. V., Hvelplund, F., Zinck, J., Sorknæs, P. Energy Storage and Smart Energy Systems. *International Journal of Sustainable Energy Planning and Managemen. 2016.* 11: 3–14. doi:10.5278/ijsepm.2016.11.2

60. Tjardo, S., Persis, D., Claudio ; Tesi, Pietro. Modeling and Control of Heat Networks With Storage: The Single-Producer Multiple-Consumer Case, IEEE Transactions on Control Systems Technology, March 2017, Vol. 25(2), pp. 414–428.

61. *Likums "Par sabiedrisko pakalpojumu regulatoriem". Koģenerācijas tarifu aprēķināšanas metodika* [tiešsaiste]. LR likums Rīga: pieņemts Rīgā 2011. gada 16. jūnijā, Latvijas Vēstnesis, interneta vietne Likumi.lv [skatīts 2020. g. 8. septembrī]. Pieejams: https://likumi.lv/ta/id/211966-kogeneracijas-tarifu-aprekinasanas-metodika

62. Žentiņš, V., Rusovs, D., Soročins, A., Decision Making Control Algorithm for Cogeneration Plants in Operating with the Heat Accumulator Deep Analysis Model. *Complex Systems Informatics and Modeling Quarterly Journal,* 2022, Riga, No. 30. ISSN: 2255-9922

63. Xu, C., Liu, M., Jiao, S., Tang, H., Yan, J., Experimental study and analytical modeling on the thermocline hot water storage tank with radial plate-type diffuser. *International Journal of Heat and Mass Transfer.* May 2022, Volume 186, 122478.

64. Fertahi, S., Jamil, A., Benbassou, A., Review on Solar Thermal Stratified Storage Tanks (STSST): Insight on stratification studies and efficiency indicators. *Solar Energy.* December 2018, Volume 176, pp. 126–145.

65. Bouzahera, M. T., Bouchahma, N., Guerirab, B., Bensacib, C., Lebbi, M. On the thermal stratification inside a spherical water storage tank during dynamic mode. *Applied Thermal Engineering.* August 2019, Volume 159, 113821.

Varis Žentiņš was born on 1 September 1987 in Jelgava. He obtained a Professional Bachelor's degree and engineer's qualification in the specialty of Heat Energy and Thermal Engineering in 2011 and a Master's degree in Thermal Energy and Heat Engineering in 2013 from Riga Technical University. From 2011 to 2018, he was an assistant project manager and project manager with "Energoremonts Rīga" Ltd. Since 2019, he has been a project manager of the construction of large industrial facilities at "Industry Service Partner" Ltd. He obtained a construction practice certificate in construction management of distribution and user gas supply systems (up to 16 bar) and construction management of heat supply, ventilation, recuperation and cooling supply systems. Since 2020, he has been a researcher with Riga Technical University. His research is related to heat storage and heat pump technologies.